176. Preparation and Structure of Oligolides from (*R*)-3-Hydroxypentanoic Acid and Comparison with the Hydroxybutanoic-Acid Derivatives: A Small Change with Large Consequences

by **Dieter Seebach***, **Torsten Hoffmann**[1]), **Florian N. M. Kühnle**[1]), and **Urs D. Lengweiler**[1])

Laboratorium für Organische Chemie der Eidgenössischen Technischen Hochschule, ETH-Zentrum, Universitätstrasse 16, CH–8092 Zürich

(4.VII.94)

Cyclic oligomers of (*R*)-3-hydroxyvaleric acid (3-HV) are prepared from the monomer by three different methods, giving various ratios of the oligomers. The macrocycles containing three to twelve 3-HV units (12- to 48-membered rings) are isolated in pure form by chromatography. The triolide **3** can be separated by distillation and isolated on large scale. *Biopol*, the copolymer of (*R*)-3-hydroxybutanoic acid (3-HB) and (*R*)-3-hydroxyvaleric acid (3-HV), is degraded to mixtures of Me- and Et-substituted triolides ('*mixolides*') with high crystallization tendency. The X-ray crystal structures of the tetrolide **4**, pentolide **5**, hexolide **6**, heptolide **7**, and of two 'mixolides' (with inclusions of solvent) have been determined (*Figs. 3–7, 10,* and *11*) and are compared with those of the corresponding 3-HB derivatives reported previously. From the structural data, a 3_1 and a 2_1 helix of 3-HV can be modelled, and the latter one compared with helix structures of P(3-HB) and P(3-HV) derived from stretch-fibre X-ray scattering. Crystals of a water-containing NaSCN complex of the triethyl triolide **3** were obtained in good quality for X-ray analysis. The structure (*Figs. 12, 13,* and *Table 6*) contains an interesting array of C=O and H_2O O-atoms around the Na^+ ions along a channel-type tube (*a*-axis of the crystal) which may be relevant to the role of P(3-HB) and P(3-HV) as components of cellular ion channels.

1. Introduction. – The biopolymer poly[(*R*)-3-hydroxybutanoic acid] (P(3-HB)) is the most important member of the family of polyhydroxyalkanoates [1] [2]. P(3-HB) has been identified by *Lemoigne* in the twenties, as a storage material in the microorganism *Bacillus megaterium* [3]. Typically, the molecular weight of this material ranges from $1–7.5 \times 10^5$ g/mol which corresponds to 2500–9000 monomeric units. The copolymer of (*R*)-3-hydroxybutanoic acid and (*R*)-3-hydroxyvaleric acid P(3-HB/3-HV), produced by fermentation with *Alcaligenes eutrophus*, is of special commercial interest and is sold under the trade name *Biopol* [4].

Besides its occurrence as microbial storage material (*s*-P(3-HB))[2]), P(3-HB) has been found in extracts from cell membranes of genetically transformable *Escherichia coli* [5]. These samples show a comparatively lower molecular weight (*ca.* 10000 g/mol or 100–150 monomeric units) and occur together with calcium polyphosphate (complexing or *c*-P(3-HB))[3]). *Reusch et al.* proposed a structure for the complex from these components (*Fig. 1, a*) which might allow for calcium ion, phosphate, or even DNA transport across the inner bacterial cell wall [5].

---

[1]) Part of the projected Ph.D. theses of *T.H.*, *F.N.M.K.*, and *U.D.L.*, ETH-Zürich.

[2]) This abbreviation has been proposed for storage P(3-HB) [1].

[3]) This abbreviation has been proposed for the low-molecular-weight P(3-HB) complexed with salts or with molecules such as $Ca \cdot PP_i$ or proteins [5b].

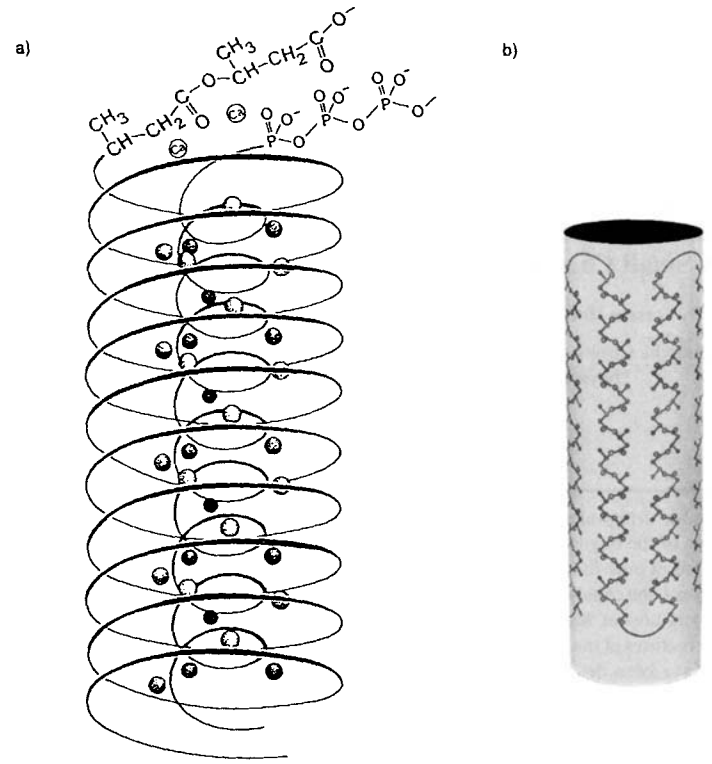

Fig. 1. a) *Structure of a [P(3-HB)Ca-PP$_i$] complex suggested by* Reusch et al. [5]. b) *An alternative channel model based on our conformation analysis of oligolide X-ray crystal structures* [7]

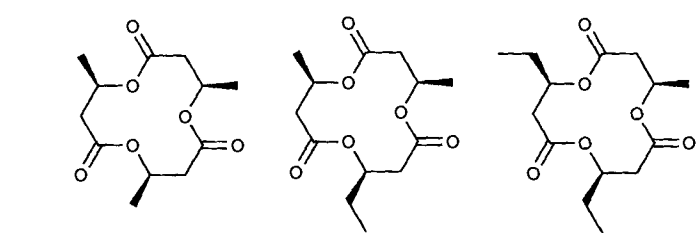

A **1** **2**

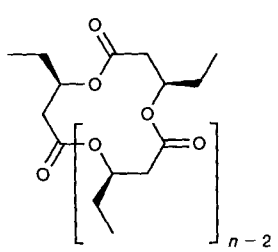

3 $n = 3$ (triolide)
4 $n = 4$ (tetrolide)
5 $n = 5$ (pentolide)
6 $n = 6$ (hexolide)
7 $n = 7$ (heptolide)
8 $n = 8$ (octolide)
9 $n = 9$ (nonolide)
10 $n = 10$ (decolide)
11 $n = 11$ (undecolide)
12 $n = 12$ (dodecolide)

During our investigations on the structure and synthesis of the proposed non-proteinogenic P(3-HB)/Ca-polyphosphate ion channel, we prepared cyclic and open-chain oligomers as model compounds [1] [6] [7]. We determined the X-ray crystal structure of several oligolides derived from 3-HB which led to the construction of a 3_1 and a 2_1 helix [1] [6]. Using the 2_1 helix as a building block, an alternative structure of the channel was proposed (*Fig. 1, b*) [7]. With the cyclic trimer **A** of 3-HB, we succeeded in crystallizing complexes of alkali-metal salts, characterized by X-ray crystal-structure analysis [8]. Several derivatives of 3-HB were used as ionophores to transport alkali and alkaline-earth picrates across a bulk liquid CH_2Cl_2 membrane [9].

In some extractions of *c*-P(3-HB) from genetically transformable *Escherichia coli* performed in our laboratories, we found P(3-HB) containing small amounts of 3-HV (*ca.* 14% by ^{1}H-NMR spectroscopy and GC of the degradation products) [10]. This discovery of 3-HV units in *c*-P(3-HB), as well as the quite different properties of *Biopol* as compared to pure P(3-HB), directed our interest towards the more lipophilic 3-HV oligomers, their structures, their complexes with ions, and their properties. Herein, we describe the preparation, isolation, and characterization of the oligolides **1**–**12** containing 3-HV units and of a sodium-thiocyanate complex with the cyclic trimer **3**.

2. Preparation and Isolation of Cyclic Oligomers from (*R*)-3-Hydroxypentanoic Acid (13). – 2.1. *Preliminary Remarks.* The preparation of these compounds can be realized in two ways. In principle, the open-chain precursor of each oligolide, the corresponding ω-hydroxy acid, is accessible by a segment-coupling method [11] and can be cyclized using well established macrolactonization reactions under high-dilution conditions [12]. The advantage of this method is the simple isolation of the desired oligolide [6]. On the other hand, mixtures of the compounds **3**–**12** should be formed in a *single* reaction, starting from (*R*)-3-hydroxypentanoic acid (**13**) itself. The crucial problem then will be the separation. We decided to follow the second approach, because, during our work on analogous compounds from (*R*)-3-hydroxybutanoic acid, we have developed suitable separation and analytical techniques [1]. Particularly, ^{13}C-NMR spectroscopy has been found to be an excellent method to determine the composition of the oligolide mixtures (see *Fig. 2, a–d*). The resonance signals of the carbonyl C-atoms appear as sharp *singlets*[4]) for each oligolide; under special measurement conditions (inverse-gated experiment), a quantitative analysis is possible. Below, we will describe different methods and conditions for preparing oligolides from (*R*)-3-hydroxypentanoic acid (**13**).

2.2. *Preparation of (R)-3-Hydroxypentanoic Acid* (**13**). As described in [13], the commercially available copolymer *Biopol* (27% 3-HV/73% 3-HB) was depolymerized in excellent yield by transesterification with MeOH under acid catalysis (conc. H_2SO_4) in boiling 1,2-dichloroethane to a mixture of the corresponding monomeric methyl esters (*Scheme 1*). These were separated by careful distillation using a *Spaltrohrkolonne*. Finally, the methyl ester of 3-HV (**13**) was saponified in a 5% aqueous solution of KOH yielding 90% of (*R*)-3-hydroxypentanoic acid (**13**) after distillation.

2.3. Yamaguchi's *Esterification Method Applied for Macrolactonization.* In 1979, *Yamaguchi* and coworkers reported a rapid and mild esterification method using mixed carboxylic 2,4,6-trichlorobenzoic anhydrides in the presence of 4-(dimethylamino)-

---

[4]) In solution, all oligolides show C_n symmetry on the NMR time scale.

Scheme 1. *Preparation of (R)-3-Hydroxyvaleric Acid* (**13**) *Starting from Biopol*

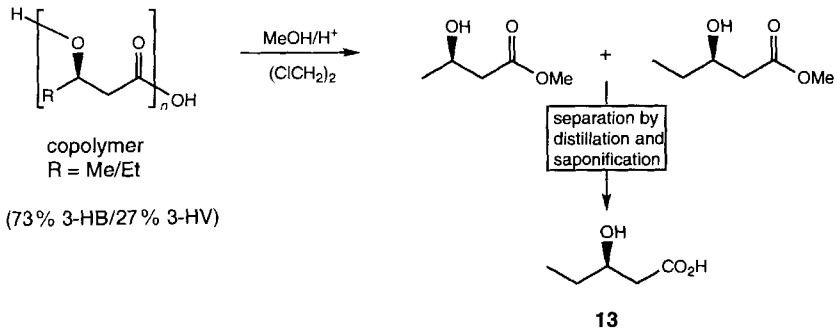

pyridine (DMAP) [14]. Under these conditions, 3-hydroxyalkanoic acids oligomerize, and eventually cyclization takes place [1] [11]. This macrolactonization consists of two steps, formation of the mixed anhydride and ring closure under high-dilution conditions. As with 3-HB [6], we followed the original procedure but preferred the cheaper 2,6-dichlorobenzoyl chloride [15] to prepare the mixed anhydride with 3-HV (**13**; *Scheme 2*). First, the lactonization step was carried out at room temperature in toluene. *Fig. 2, a,* shows the ^{13}C-NMR spectrum of the crude oligolide mixture after basic workup. As can be seen, mainly oligolides containing 5–8 units were formed. The major product is the pentolide **5** (35%), followed by hexolide **6** (27%), heptolide **7** (15%), and octolide **8** (8%). Only minor amounts of the triolide **3**, tetrolide **4** as well as of the 'higher' oligolides **9**–**12** were present in the reaction mixture. In a second run, the lactonization step was carried out in refluxing benzene, and the reaction time was prolonged. The total yield decreased (from 80 to 35%; the side reaction is elimination of H_2O to give pent-2-enoic acid), but now there were also the smaller rings: main products were still the pentolide **5** (46%) and the hexolide **6** (24%), besides which the tetrolide **4** (9%) and even the triolide **3** (5%) were formed. Obviously, DMAP in refluxing benzene is capable of cleaving ester bonds [16], and smaller cycles become entropically preferred.

Scheme 2. *Preparation of Macrocycles* **3**–**12** *According to the Method of* Yamaguchi (*A*), *the DCC-Activated Lactonization* (*B*), *and to the Acid-Catalyzed Lactonization* (*C*)

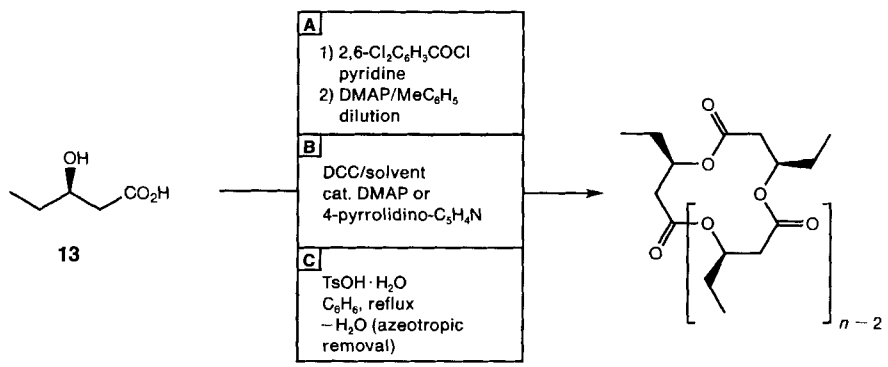

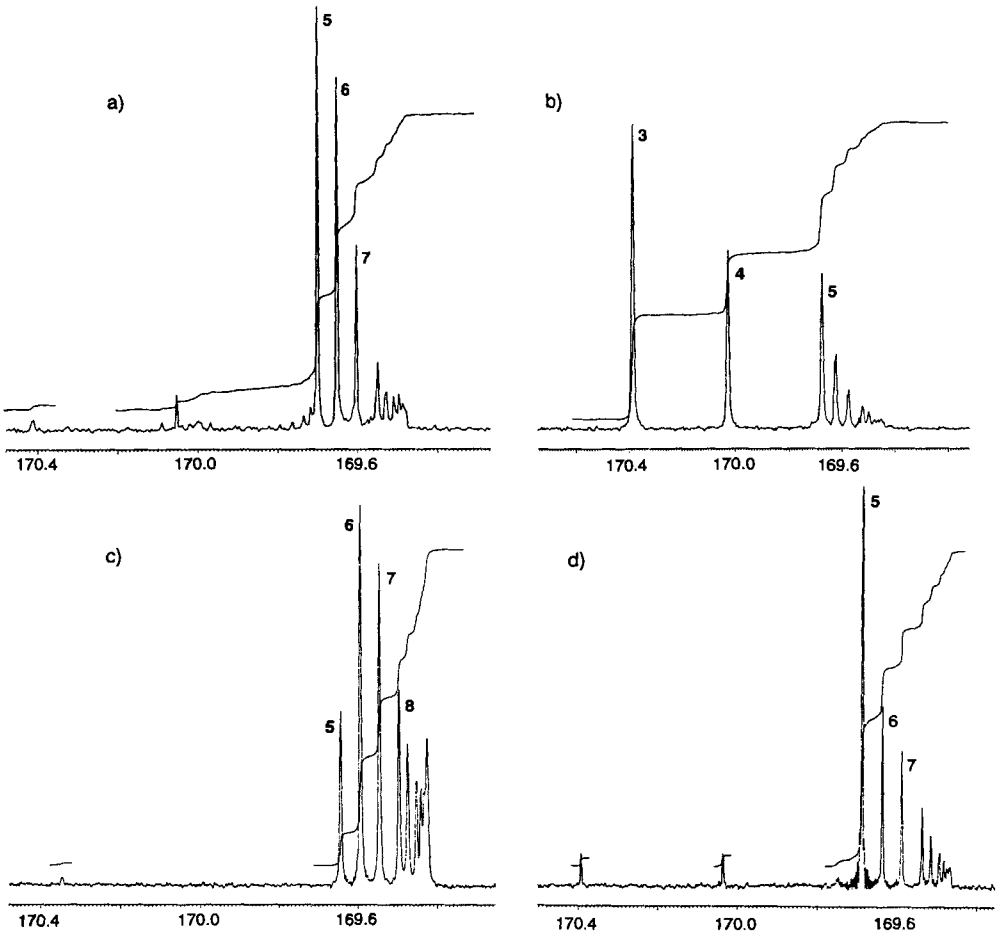

Fig. 2. *'Quantitative' ^{13}C-NMR spectra of the C=O region of oligolide mixtures obtained from* **13** *by* a) Yamaguchi's *method in toluene at r.t.,* b) *acid catalysis with $TsOH \cdot H_2O$ in benzene at reflux,* c) *DCC-activated lactonization in CCl_4 at 0°,* d) *DCC-activated lactonization in CH_2Cl_2 at 0°*

2.4. N,N'-*Dicyclohexylcarbodiimide (DCC)-Induced Lactonization.* In the presence of carbodiimides, equimolar mixtures of carbocylic acids and alcohols undergo condensation to esters in high yields [17]. In some cases, this procedure failed: fatty acids and alcohols give *N*-acylureas in the presence of DCC [18]. By the work of *Neises* and *Steglich* [19], a modification of the esterification procedure has been introduced, which consists of the addition of catalytic amounts of a 4-(dialkylamino)pyridine to the mixture of carboxylic acid, alcohol, and carbodiimide. If the carboxylic acid contains an additional OH group, the structure of the products will depend on the relative positions of these two functional groups. Years ago, *Woodward et al.* [20] demonstrated lactone formation in their total synthesis of reserpine, which encouraged us to use DCC as esterification/lactonization reagent. We first chose Et_2O as solvent, DMAP as catalyst, and DCC as

activating reagent. The reaction was carried out at room temperature with a 0.1-mol/l concentration of the monomeric acid **13**. To our surprise, cyclic oligomers were formed in *ca.* 90% yield; no open-chain polymers could be detected in the crude product! The distribution (determined by quantitative ^{13}C-NMR spectroscopy) of oligolides **3**–**12** is given in *Table 1* (*Entry 1*). The hexolide **6** (a 24-membered ring) was the main product, followed by pentolide **5**, heptolide **7**, and the 'higher' oligolides **8**–**12**. Triolide **3** could not be detected, and the tetrolide **4** was formed in only 1% yield. We then optimized the

Table 1. *Oligolide Distributions* ([%]) *of Macrolides* **3**–**12** (containing 3–12 3-HV units), *as Determined by 'Quantitative' ^{13}C-NMR Spectroscopy*. 0 stands for < 1%.

Entry	Conditions	Conc. of **13** [mol/l]	**3**	**4**	**5**	**6**	**7**	**8**	**9**	**10**	**11**	**12**
1	Et_2O, DMAP, r.t., DCC	0.1	0	1	20	31	16	11	7	6	5	3
2	Et_2O, 4-pypy, r.t., DCC	0.1	0	0	15	31	19	13	9	6	4	3
3	Et_2O, 4-pypy, r.t., DCC	0.04	0	1	20	32	18	12	7	5	3	2
4	Et_2O, 4-pypy, r.t., DCC	0.5	2	2	16	23	17	15	11	7	5	2
5	Et_2O, 4-pypy, r.t., DCC	1.0	1	1	24	24	17	12	8	6	4	3
6	Et_2O, 4-pypy, 0°, DCC	0.04	0	0	19	30	19	12	8	5	4	3
7	Et_2O, 4-pypy, 0°, DCC	0.5	1	0	23	29	19	14	7	4	2	1
8	Et_2O, 4-pypy, 0°, DCC	1.0	2	1	26	29	18	13	6	3	1	1
9	Et_2O, DMAP, r.t., DIC	0.1	0	1	20	27	15	10	9	8	6	4
10	Et_2O, 4-pypy, r.t., DIC	0.1	0	1	20	27	16	11	9	8	5	3
11	Et_2O, DMAP, 0°, DIC	0.1	0	0	21	31	19	12	8	4	3	2
12	EtO, DMAP, 0°, DIC	0.5	1	1	28	27	19	13	6	3	1	1
13	PhMe, 4-pypy, r.t., DCC	0.1	1	1	27	26	15	10	8	6	4	2
14	CH_2Cl_2, 4-pypy, r.t., DCC	0.1	7	6	50	15	9	5	4	3	1	0
15	CH_2Cl_2, 4-pypy, 0°, DCC	0.1	3	3	47	17	11	8	5	3	2	1
16	MeCN, 4-pypy, 0°, DCC	0.1	7	4	52	13	10	7	3	2	1	1
17	CCl_4, 4-pypy, r.t., DCC	0.1	0	0	13	30	19	13	9	7	5	4
18	CCl_4, 4-pypy, 0°, DCC	0.1	0	0	11	27	20	14	9	8	6	5
19	CCl_4, 4-pypy, 0°, DCC	0.5	0	1	15	29	19	13	9	7	4	3
20	CCl_4, 4-pypy, −20°, DCC	0.1	0	0	9	23	23	15	9	8	7	6

carbodiimide-activated reaction towards the preparation of oligolides containing six and more monomeric units. First, we replaced DMAP by 4-pyrrolidinopyridine (4-pypy), which is known as a very efficient nucleophilic catalyst for esterifications at room temperature [21] (*Entry 2*). Indeed, the amount of the pentamer **5** decreased in favor of the total yield of **7**–**12**. Hexamer **6** was still found as the main product. This means that the relative rate of chain growth by esterification increases, while the lactonization of the activated open-chain precursor still takes place, but now with formation of 'higher' cyclic oligomers. What will happen, if we change the initial concentration of the monomeric hydroxy acid **13**? *Entry 3* shows the oligolide distribution for $c = 0.04$ mol/l under the same conditions as in *Entry 2*. Now, the amount of pentamer **5** increased again at the expense of the 'higher' oligomers **7**–**12**. This means a decelerated rate of chain growth in comparison with the lactonization step. Interestingly, *Entries 1* and *3* gave nearly the same oligolide distributions for $n = 5$–8. When we raised the concentration of **13** up to 0.5 mol/l (*Entry 4*) or even 1.0 mol/l (*Entry 5*), still *ca.* 90% of the crude product contained cyclic oligomers! With increasing concentration of **13**, the formation of oligolides, con-

taining 7–12 units, increased as well; but when a certain concentration is exceeded, lactonization to smaller rings occurs. In our experiments (Et_2O as solvent), a concentration of 0.1 mol/l for **13** gave the highest yield of oligolides with $n \geqslant 7$. In a next optimizing step, we reduced the reaction temperature to 0° under otherwise identical conditions (*Entries 6, 7,* and *8*). In comparison to the corresponding runs at room temperature with the same initial concentrations of **13**, the changes in the oligolide distributions are rather small. However, another important effect should be mentioned at this point. At room temperature *ca.* 5% of the product consists of *N*-acylated ureas, which could be avoided at 0° (merely *ca.* 1%)[5]).

Numerous investigations have shown that the rate of the reaction of carbodiimides with carboxylic acids and the ratio of the products obtained are influenced by the type of carbodiimide used [22]. Therefore, we investigated the effect of *N,N'*-diisopropylcarbodiimide (DIC)[6]) on the product ratio (*Entry 9*). As can be seen, the use of DIC instead of DCC did not lead to a significant increase of the higher oligolides. These are formed in comparable ratios, and the hexolide **6** remains to be the main product. Also with DIC as activating reagent, the catalyst, the concentration of the hydroxy acid **13**, and the reaction temperature were varied (*Entries 10, 11,* and *12*). The composition of the oligolide mixtures showed the same tendencies as we have found with DCC.

Solvents exert a strong effect on the reaction rate of carbodiimides with carboxylic acids [23]. In our case, an enormous consequence on the oligolide composition was observed (*Entries 13–17*). In comparison with the corresponding reactions in Et_2O, the following results were obtained: in toluene nearly twice as much pentolide **5** is formed, followed by hexolide **6** and the oligolides **7**–**12**. In CH_2Cl_2 and MeCN, *ca.* 50% of pentolide **5** are detected. Most important 'side product' is the hexolide **6**. The quantitative ^{13}C-NMR spectrum of the crude product mixture obtained as specified in *Entry 15* is shown in *Fig. 2, d.* This means that – starting from **13** – the 20-membered oligolide **5** is prepared in only one step and in a yield of 50%. The amount of oligolides with $n \geqslant 6$ was found to be largest in CCl_4. The optimized conditions are given in *Entry 18*. Here, the yields of the hexolide **6**, heptolide **7**, and also of the octolide **8** are higher than that of pentolide **5**. The quantitative ^{13}C-NMR spectrum of this run is shown in *Fig. 2, c.* Finally, the ratio can be improved by reducing the temperature (−20°; *Entry 20*). But in most cases, we preferred a reaction temperature of 0°, because at −20° the reaction time is drastically increased (150 h, *ca.* 90% cyclic products). In several experiments, we investigated whether (*R*)-3-hydroxybutanoic acid can be converted to similar mixtures of macrocycles, which is indeed observed (for a discussion, see *Sect. 2.8*).

2.5. *Acid-Catalyzed Lactonization.* As early as 1934, *Stoll* and *Rouvé* [24] published the macrolactonization of 15-hydroxypentadecanoic acid and 16-hydroxyhexadecanoic acid with benzenesulfonic acid to the 16- and 17-membered rings in high yields. We applied a similar procedure, but replaced the catalyst by $TsOH \cdot H_2O$ (*cf.* previous work with 3-HB [6] [25]). The quantitative ^{13}C-NMR spectrum of an oligolide mixture, isolated from a reaction in boiling benzene after 48 h, is shown in *Fig. 2, b.* Here, the formation of the triolide **3** (40%) is favored. Besides, we obtained the tetrolide **4** (20%), pentolide **5** (20%), and the hexolide **6** (10%). Only small amounts (12% overall) of higher cyclic

---

[5]) Except with MeCN as solvent, which leads to a larger amount of *N*-acylated ureas.

[6]) Advantageously, the resulting urea is water-soluble and is removed during workup.

oligomers could be detected in the spectrum, but we never tried to isolate them. In a next step, we changed the solvent (toluene/1,2-dichloroethane 4:1) to increase the reaction temperature, hoping to isolate larger amounts of the lower oligolides in analogy to the finding with *Yamaguchi*'s method. In fact, the composition of the crude reaction mixture clearly changed: we now obtained much more triolide **3** (56%), less tetrolide **4** (11%), pentolide **5** (18%), and hexolide **6** (8%), indicating that the formation of the triolide **3** is thermodynamically preferred. On the other hand, H_2O elimination to the $\alpha\beta$-unsaturated acid occurs as side reaction at these higher temperatures. Thus, the relative yield of triolide **3** increased, but the absolute amount remained nearly the same.

2.6. *Separation and Isolation of the Macrolides* **3**–**12**. Oligolides obtained by *Yamaguchi*'s method or the DCC-activated reaction can be separated into mixed fractions by flash chromatography (silica gel; pentane/Et_2O 2:1). Pentolide **5** and triolide **3** are eluted first, followed by a mixed fraction containing tetrolide **4** and hexolide **6**. The next fraction contains heptolide **7** and octolide **8**. To elute nonolide **9**, decolide **10**, undecolide **11**, and dodecolide **12** in this order, the polarity of the solvent is increased (pentane/Et_2O 1:1); still, each oligolide is obtained in a mixed fraction with the following one. Only a rather small amount (*ca.* 5–10%) is isolated in pure form. Separations of mixtures **9**/**10**, **10**/**11**, and **11**/**12** could be achieved by repeated flash chromatography (silica gel; pentane/Et_2O 1:1) or by the use of a multibore column [26]. Pentolide **5** and triolide **3** can be isolated by flash chromatography (silica gel; toluene/Et_2O 3:1). Hexolide **6** can be separated from tetrolide **4** by repeated fractional crystallization from hexanes/CH_2Cl_2 or by flash chromatography (silica gel; CH_2Cl_2/Et_2O 20:1). The most difficult separation was that of heptolide **7** and octolide **8**. Attempts using flash chromatography with several eluents or crystallization methods failed. It turned out that only repeated medium-pressure liquid chromatography (MPLC) or preparative high-pressure liquid chromatography (HPLC) leads to the pure compounds **7** and **8**. Oligolides obtained by the acid-catalyzed lactonization can be isolated up to the hexamer **6** by the procedure described above. But, advantageously, the crude product is purified by bulb-to-bulb distillation, to isolate the triolide **3**, which can be recrystallized from pentane. Then, the distillation residue is separated as described above. Oligolides **3**–**12** have been isolated and characterized by IR, ^{1}H-NMR and ^{13}C-NMR spectroscopy, liquid-secondary-ionization mass spectroscopy (LSI-MS), specific rotation, elemental analysis, and osmometric molecular-weight determination[7]).

2.7. *Preparation of the Mixed Triolides* **1** *and* **2**. Since we have found a remarkably simple way of preparing the triolide **A** directly from P(3-HB) on a 20-g scale [6] [25], we treated the cheaper copolymer *Biopol* (73% 3-HB/27% 3-HV) under the same conditions: the copolymer was dissolved in toluene/1,2-dichloroethane 4:1 and heated at reflux in the presence of $TsOH \cdot H_2O$. After basic workup and distillation of the residue, a mixture of triolides **A**, **1**, **2**, and **3** was obtained in 25–35% yield. To our surprise, the mixture containing four different compounds was a material of extremely high crystal-

[7]) These values differ sometimes considerably from the calculated ones. But, an osmometric molecular-weight determination (for instance 1000 ± 100 g/mol) immediately establishes purity: had there been an equivalent of a small molecule (*e.g.* H_2O) as impurity within the oligolide, the apparent molecular weight would have been *ca.* half the observed value!

Scheme 3. *Preparation of* Mixolides, *Containing Either 73% 3-HB/27% 3-HV or 33% 3-HB/67% 3-HV*. The flask shows crystals of the four-component mixture **A**/**1**/**2**/**3** which formed spontaneously in the receiver flask of the vacuum distillation apparatus.

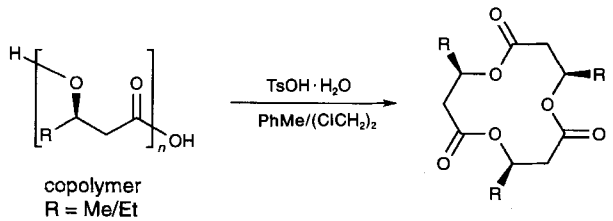

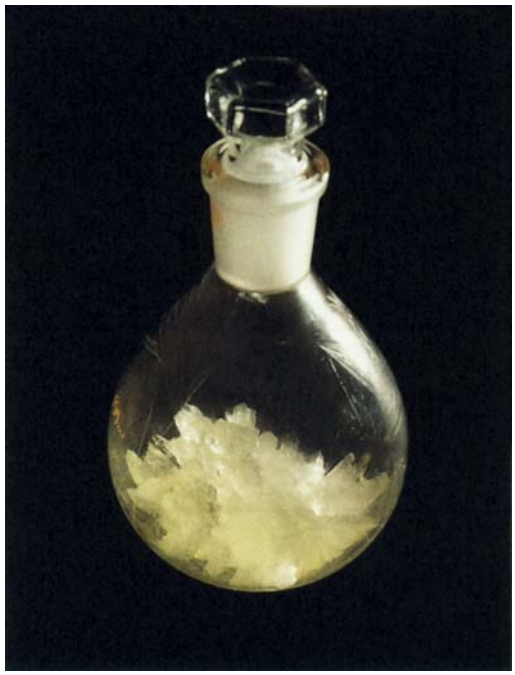

lization tendency (see *Scheme 3*). The quantitative ^{13}C-NMR spectrum (C=O region) of this mixture had the following composition: **A** (38%), **1** (44%), **2** (16%), and **3** (2%), as expected from a statistical calculation (**A** (39%), **1** (43%), **2** (16%), and **3** (2%)).

To see what happens when we increase the content of Et *vs.* Me groups in the *mixolide*, we have also prepared a *mixolide* from *Biopol* (73% 3-HB/27% 3-HV) and 3-HV (**13**; total content of 3-HV units 66.7%) under the same conditions as described above. A mixture of triolides **A**, **1**, **2**, and **3** was obtained in *ca.* 38%. The quantitative ^{13}C-NMR spectrum (C=O region) showed the following composition: **A** (2%), **1** (20%), **2** (46%), and **3** (32%) (statistical values: **A** (4%), **1** (22%), **2** (44%), and **3** (30%)). These compounds could be separated by repeated flash chromatography (silica gel; pentane/Et_2O 3:1). The pure triolides **1** and **2** with one and two Et groups, respectively, were isolated and fully characterized.

2.8. *Comparison of the Oligolides* **3–12** *with Their 3-HB Analogs from the Synthetic Point of View. a*) Macrolides obtained by *Yamaguchi*'s method at room temperature showed in the case of 3-HV (**13**) as starting material a clear preference for the formation of oligolides containing five and more monomeric units. Main product is the pentolide **5** (35%), followed by hexolide **6** (27%), heptolide **7** (15%), and the octolide **8** (8%). Under the same conditions with 3-HB as monomeric building block, the corresponding hexolide was formed as the main product (29%), and the pentolide was only second (22% yield), indicating that the oligolides of 3-HB with $n \geqslant 7$ were formed in larger amounts. In refluxing benzene and with prolonged reaction times, the total yield of oligolides derived from 3-HV (**13**) decreased. Main products were still the pentolide **5** (46%) and the hexolide **6** (24%). When the reaction temperature and time were increased even more, the same behavior could be observed with 3-HB as starting material.

b) The DCC-induced lactonization of 3-HV (**13**) was found to be dependent upon the type of carbodiimide, the catalyst, the concentration of the hydroxy acid, the reaction temperature, and, significantly so, upon the kind of solvent used. In a comparison with 3-HB as starting material, we observed that the obtained oligolide distributions (see *Table 2* and also *Table 1*) differed enormously from those observed in the corresponding runs with 3-HV (**13**).

Table 2. *Oligolide Distributions* ([%]) *of Macrolides Containing 3–12 3-HB* (*n*) *Units, as Determined by 'Quantitative' ^{13}C-NMR Spectroscopy.* 0 stands for < 1%.

Entry	Conditions	Conc. of 3-HB [mol/l]	3	4	5	6	7	8	9	10	11	12
1	Et_2O, 4-pypy, 0°, DCC	0.1	1	0	16	37	23	14	6	2	1	0
2	CH_2Cl_2, 4-pypy, 0°, DCC	0.1	6	2	35	18	16	9	6	4	3	1
3	$(CH_2Cl)_2$, 4-pypy, 0°, DCC	0.1	4	3	29	17	15	11	8	7	4	2
4	CCl_4, 4-pypy, 0°, DCC	0.1	0	0	5	28	22	16	11	9	5	4

c) The acid-catalyzed lactonization of 3-HB in comparison with 3-HV (**13**) led to rather similar amounts of the corresponding oligolides. As main products appeared in both cases the triolides, reflecting the remarkable thermodynamical preference for the 12-membered ring under these conditions.

3. Crystallizations and X-Ray Crystal-Structure Analyses. – 3.1. *General Remarks.* Compared to the results of previous structural investigations on 3-HB derivatives [1] [6] [8] [25] [27], the oligolides of 3-HV (**13**) show a distinctly poorer crystallization tendency. Only the pentolide **5** gave suitable crystals for X-ray structure analysis by simple recrystallization from a 1:1 mixture of Et_2O/pentane. The hexolide **6** gave two different crystal modifications upon recrystallization from hexanes. The dominating one was a cotton like bunch of very fine long needles, with a tendency to cover and include very few rectangular single crystals. The tetrolide **4** and the heptolide **7** could not be crystallized from common solvents, neither by cooling nor by evaporation methods. They both were isolated as oils and crystallized after standing for several months at room temperature. These difficulties to obtain single crystals may be explained by the additional degree of freedom, the rotation of the Et groups, which also caused disorder phenomena in the pentolide **5** and heptolide **7** structures (responsible for the relatively high *R* factor (*cf. Table 3*).

Table 3. *Crystal Data for the Pure 3-HV Oligolides* **4–6** *and for the Two* Mixolides

Compound	Tetrolide **4**	Pentolide **5**	Hexolide **6**	Heptolide **7**	Na-complex	*Mixolide* 27% HV	*Mixolide* 67% HV
Formula	$C_{20}H_{32}O_8$	$C_{25}H_{40}O_{10}$	$C_{30}H_{48}O_{12}$	$C_{35}H_{56}O_{14}$	$C_{17}H_{29.5}N_{1.5}NaO_8S$	$C_{15}H_{25}O_{6.5}$	$C_{15}H_{24.5}O_{6.25}$
Molecular weight	400.4	500.5	600.7	700.8	438.0	309.4	304.9
Space group	$C2$	$P2_1$	$P2_12_12_1$	$P2_1$	$P2_12_12_1$	$C222_1$	$C222_1$
a [Å]	20.521(4)	10.95(2)	8.351(2)	10.499(1)	11.694(4)	16.137(3)	16.021(3)
b [Å]	5.616(1)	9.42(2)	15.555(3)	10.248(1)	16.097(10)	20.913(4)	21.236(9)
c [Å]	20.335(4)	14.27(3)	25.653(5)	18.513(1)	24.892(8)	9.641(2)	9.750(5)
β [°]	107.6(3)	103.9(3)		99.4(1)			
V [Å^3]	2232.8	1429.0	3332.3	1965.1	4685.7	3253.6	3317.6
Z	4	2	4	2	8	8	8
ϱ calc. [gcm^{-3}]	1.19	1.16	1.20	1.18	1.24	1.26	1.22
$F(000)$	864	530	1296	756	1860	1336	1232
μ [mm^{-1}]	0.091	0.089	0.092	0.091	0.20	0.096	0.75
Range measured	2–25	1.5–22.5	0–25	1.5–25	2–25	0–25	2–63
Scan type	ω	2θ–θ	ω	ω	ω	ω	$\omega/2\theta$
Reflections measured	2191	1447	3310	3673	4576	1623	1194
Reflections used	$> 4\sigma[F]$: 1356	$> 6\sigma[F]$: 962	$> 4\sigma[F]$: 2609	$> 4\sigma[F]$: 2395	$> 4\sigma[F]$: 2731	$> 4\sigma[F]$: 1025	$> 4\sigma[F]$: 966
No. of parameters	254	331	379	440	499	187	192
Final R (unweighted)	0.097	0.054	0.064	0.073	0.055	0.076	0.083

3.2. *Crystal Structures of* **4–7**. The tetrolide **4** (*Fig. 3*) crystallizes, as the 3-HB analogue, in the centered space group C_2, but in this case the unit cell contains two molecules, because the crystallographic C_2 symmetry is destroyed by the position of the Et groups in the 3-HV analog **4**. In spite of this, the best fit for the ring atoms of the 3-HB and 3-HV tetrolides, including the carbonyl O-atoms and the Et CH_2 groups, is almost perfect.

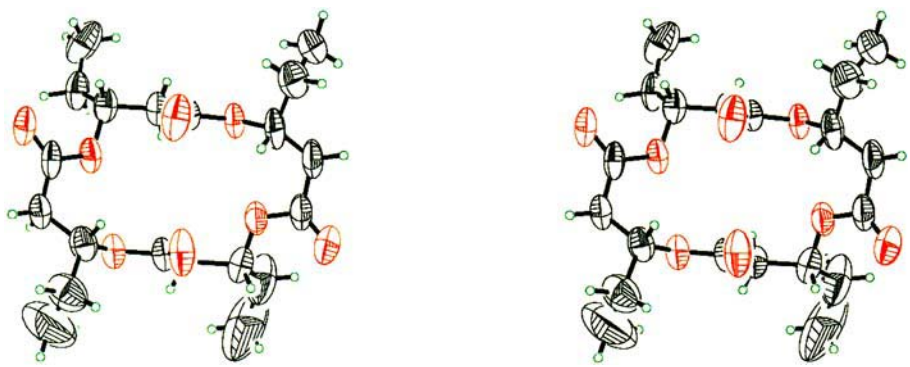

Fig. 3. *ORTEP Stereoview of the crystal structure of* **4**. O-Atoms are indicated in red, C-atoms in black, H-atoms in green. Vibrational ellipsoids for the non-H-atoms are drawn at the 50% probability level. The relatively large thermal displacement parameters of the Me groups are responsible for the high R factor.

The pentolide **5** (*Fig. 4*) crystallizes in the monoclinic space group $P2_1$. The molecule adopts a rather flat disk-like conformation with four carbonyl O-atoms on one and the fifth on the opposite side of the mean molecular plane. Four of the five Et groups are in a *quasi*-equatorial position. The agreement in the best fit of the ring atoms for the pentolide **5** and its 3-HB analogue (*cf. Fig. 7*) is not nearly as perfect as in the tetrolide **4**.

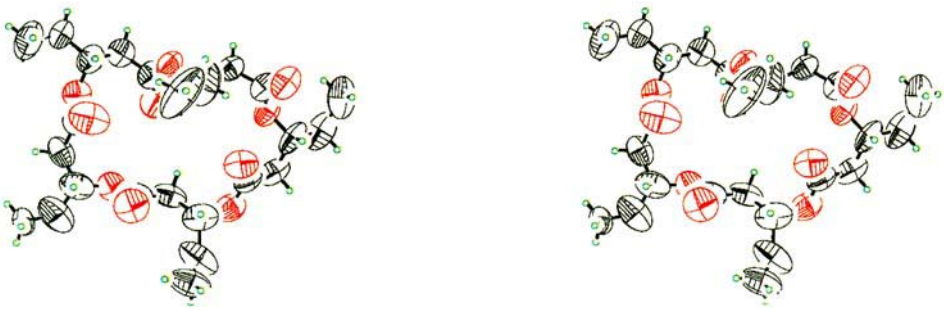

Fig. 4. *ORTEP Stereoview of the crystal structure of* **5**. O-Atoms are indicated in red, C-atoms in black, H-atoms in green. Vibrational ellipsoides for the non-H-atoms are drawn at the 50% probability level. The rest-electron-density peaks are omitted for clarity.

In the crystal structure, the hexolide **6** (*Fig. 5*) has five of the six 3-HV units in a mean molecular plane. The sixth 3-HV unit is perpendicular to this mean plane. The overall structure of **6** is strikingly different from the 3-HB hexolide. All attempts to find a best fit for the two backbones failed. However, two substructures are present in both molecules: one of them has the shape of a *A*, the other one resembles the letter S. These two fragments occurred several times in different 3-HB oligolide structures and could be used to model a 2_1 and a 3_1 helix [6] (see the discussion in *Chapt. 3.3*).

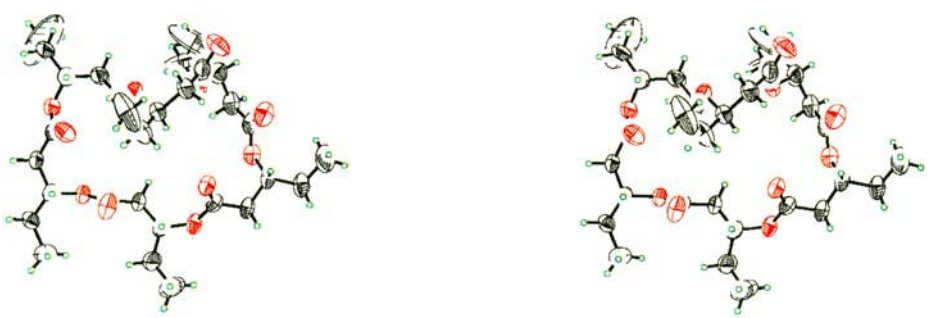

Fig. 5. *ORTEP Stereoview of the crystal structure of* **6**. O-Atoms are indicated in red, C-atoms in black, H-atoms in green. Vibrational ellipsoides for the non-H-atoms are drawn at the 50% probability level. The structure of **6** is the first of the 3-HV structures to show ring folding. The disorder of two Me groups can be seen from their anisotropic displacement parameters.

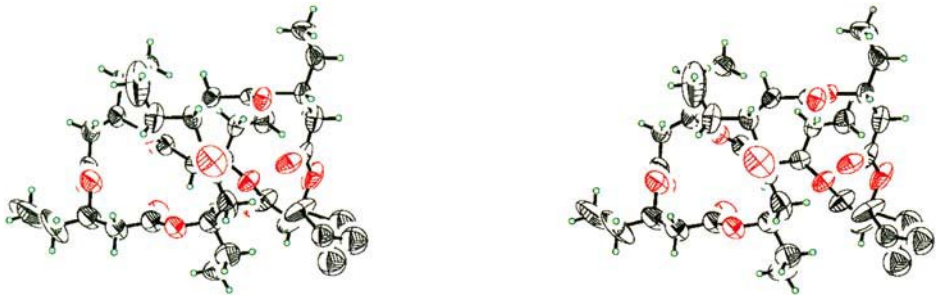

Fig. 6. *ORTEP Stereoview of the crystal structure of* **7**. O-Atoms are indicated in red, C-atoms in black, H-atoms in green. Vibrational ellipsoides for the non-H-atoms are drawn at the 50% probability level. The disorder of one Et group is resolved to two semi-occupied positions, which were refined anisotropically.

In the heptolide **7** structure (*Fig. 6*), the degree of ring folding is even greater: a mean molecular plane can still be recognized, but it contains only four of the seven 3-HV units, the other three being located over and above this plane and forming a *Δ* fragment as observed in the hexolide **6**. The overall similarity with the 3-HB heptolide is greater than in the case of the hexolides. The similarities and differences of 3-HB and 3-HV derivatives are clearly recognized by inspection of *Fig. 7* in which we have superimposed best fits of the oligolide backbones (3-HB in black, 3-HV in red).

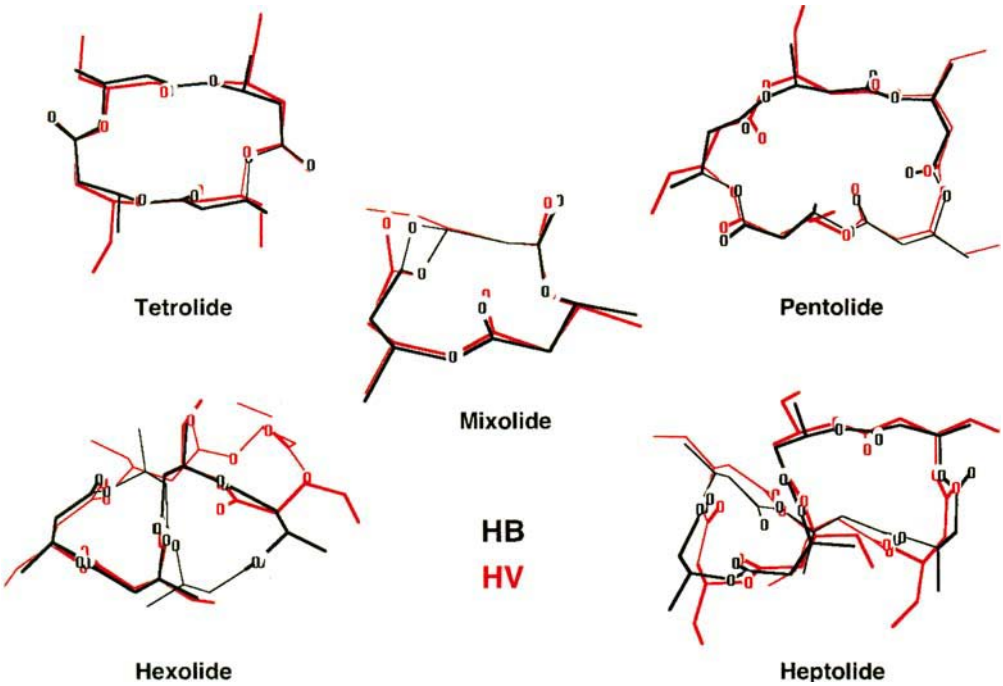

Fig. 7. *Superposition of the 3-HV oligolides* **4**–**7** *and of the* mixolide *27% 3-HV with their 3-HB analogue*. The 3-HV oligolides are indicated in red, the 3-HB derivatives in black. The structural presentations in this figure were generated from the crystal coordinates using the MacMoMo program by *Max Dobler* (Laboratorium für Organische Chemie, ETH-Zürich).

3.3. *Conformation Analysis of the Oligolides* **4**–**7**. From the four crystal structures described above, we can extract the torison angles τ_1, τ_2, τ_3, and τ_4 around the four single bonds of each 3-HV unit (22 altogether; see *Tables 4* and *5*). As in the oligo(3-HB)

Table 4. *Torsion Angles in the 3-HV Oligolide X-Ray Crystal Structures*

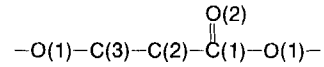

Compound	*n*	τ_1	τ_2	τ_3	τ_4	Conformation
Tetrolide **4**	1	148.8	−75.3	49.5[a])	−178.3	
	2	155.1	−70.9	176.7	−177.5	
	3	146.7	−71.9	47.1[a])	179.9	
	4	155.1	−70.0	178.4	179.5	
Pentolide **5**	1	131.0	−63.8	173.5	−172.7	
	2	84.8[a])	−167.8[a])	−160.5[a])	178.7	
	3	136.5	−68.0	151.3	178.1	
	4	111.6	−68.7	151.3	178.1	
	5	92.0[a])	−175.8[a])	88.5[a])	−164.4	
Hexolide **6**	1	96.7[a])	−70.6	−77.8[a])	−178.6	S
	2	126.9	−69.6	148.7	−179.8	
	3	86.2[a])	−166.9[a])	−144.9[a])	166.7	*Δ*
	4	136.8	−60.1	152.4	−176.4	*Δ*
	5	135.0	−59.4	160.6	−168.4	*Δ*
	6	134.8	−59.8	−22.5	−179.3	S
Heptolide **7**	1	137.2	−65.5	170.7	−179.8	*Δ*
	2	141.8	−61.0	−35.6	−175.3	S
	3	132.7	−64.6	151.8	−177.9	
	4	127.5	−64.5	176.8	−171.8	
	5	142.1	−63.5	−9.6	177.9	S
	6	132.8	−177.4[a])	−145.4[a])	−176.2	*Δ*
	7	132.1	−51.3	126.5	178.8	*Δ*
Average		136.9	−65.5	*Δ*: 159.4	176.2	
Standard deviation		10.2	5.6	*Δ*: 15.5	4.4	

[a]) These torsion angles were not taken into account in the statistics, because they were considered to be 'outliners'.

Table 5. *Averaged Bond Lengths and Bond Angles for Δ- and S-Type Structural Fragments in* **4**–**7**. Standard deviations are given in parentheses. Torsion angles are averaged for the *Δ* fragment. For the S fragment, the torsion angles derived from the hexolide **6** are shown.

Bond length		Bond angle	
O(1)−C(3)	1.455 (0.022)	C(1)−O(1)−C(3)	118.2 (1.3)
O(1)−C(1)	1.333 (0.012)	O(1)−C(1)−C(2)	111.3 (1.7)
C(1)−O(2)	1.197 (0.013)	O(2)−C(1)−C(2)	125.2 (2.0)
C(1)−C(2)	1.489 (0.019)	C(1)−C(2)−C(3)	114.5 (1.9)
C(2)−C(3)	1.505 (0.034)	C(2)−C(3)−O(1)	106.2 (1.9)
C(3)−C(4)	1.503 (0.028)	C(2)−C(3)−C(4)	114.0 (2.7)
C(4)−C(5)	1.475 (0.061)	C(3)−C(4)−C(5)	117.0 (6.2)

Torsion angle	*Δ* Type	S Type	Torsion angle	*Δ* Type	S Type
C(3)−O(1)−C(1)−C(2)	−176.2 (4.4)	−179.3	C(1)−C(2)−C(3)−O(1)	−65.5 (5.7)	−59.8
O(1)−C(1)−C(2)−C(3)	159.4 (15.5)	−22.5	C(2)−C(3)−O(1)−C(1)	136.9 (10.2)	134.8

structures, there appear to be two conformational minima for τ_3, the dihedral angle for the α-carbonyl C–C bond. The smaller one (−22°) occurs in the S, the larger one (+159°) in the Δ fragments. The S fragments in the hexolide **6** and heptolide **7** provide us with only four values of the smaller τ_3 angle while all other substructures contain the large τ_3 angle (a total of 12). Using the S fragment of **6**, we can construct a 2_1 helix for P(3-HV) shown and compared with the corresponding P(3-HB) helix [6] in *Fig. 8*. As can be seen, the pitch of the two helices is quite different (5.6 *vs.* 6.1 Å) and both agree with the structures derived from stretch-fibre X-ray diffraction measurements (5.6 *vs.* 6.0 Å) [28] [29]. The

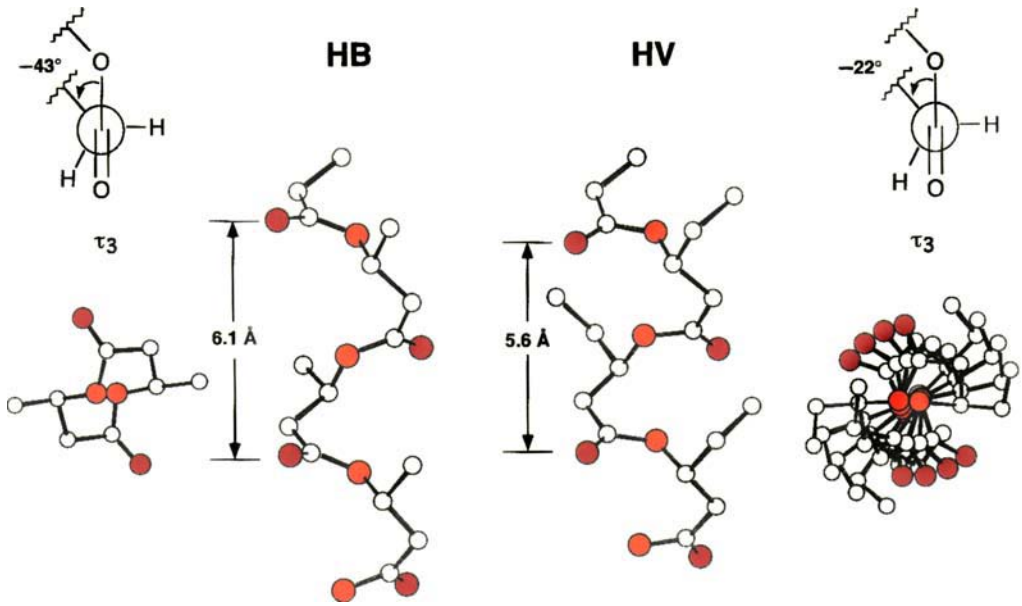

Fig. 8. *Left-handed 2_1 helices, constructed with the torsion angles of the* S *fragment of the hexolide* **6**, *listed in* Table 4. On the basis of the crystallographic designation of screw axes, the helix symmetry is expressed in the form N_m, which implies that a motif repeats after rotation about an axis by $2\pi/N$, plus a translation parallel to the screw axis of m/N times the repeat in that direction. Although a 2_1 screw axis has no chirality sense, we find in our case a left-handed or *M* helicity by following the P(3-HB) backbone. This classification differs from the nomenclature used in protein chemistry: in an N_m helix, *N* denotes the number of amino acids per rotation and *m* the number of atoms of the ring formed through a H-bond and its associated chain segment.

3-HV 3_1 helix, modelled with the average angles τ_1, τ_2, τ_4, and the larger τ_3 value, is shown and compared with the 3-HB 3_1 helix in *Fig. 9*. The 3-HV deviates more than the 3-HB helix from an ideal 3_1 helix. As has been pointed out before, a 3_1-type helix of P(3-HB) has not been found experimentally. The somewhat different torsion angles in the 3-HB and 3-HV units lead again to different pitches of the corresponding '3_1' helices. This time, the 3-HV-derived helix is steeper than the HB-derived one (6.7 *vs.* 6.0 Å).

3.4. *Crystal Structure of Mixtures of Triolides* **A**, **1**, **2**, *and* **3**. To our surprise, a mixture of 38% **A**, 44% **1**, 16% **2**, and 2% **3** (percentages determined by quantitative ^{13}C-NMR) crystallized after distillation (see *Scheme 3*), while we have so far not been able to isolate single crystals of the pure triethyl triolide **3**! Crystals suitable for X-ray structure analysis

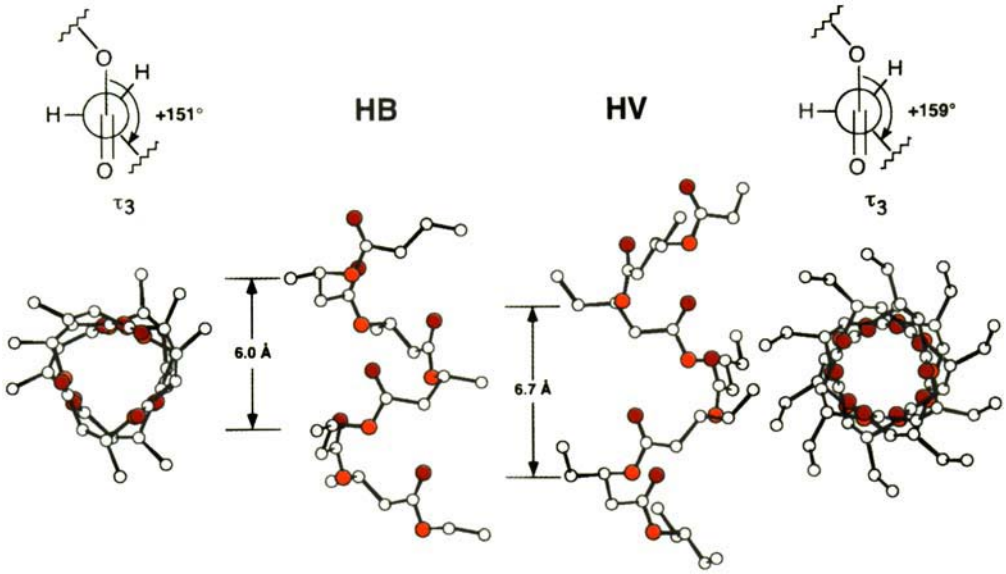

Fig. 9. *Right-handed 3_1 helices, constructed with the averaged torsion angles of the Δ fragment, listed in* Table 4

of the *mixolide* could be obtained by simple recrystallization from a pentane/Et_2O mixture 4:1 without alteration of its composition. The orthorhombic crystals (space group $C222_1$) include solvent molecules which could be identified as Et_2O by ^{1}H-NMR spectroscopy. The asymmetric unit of the unit cell contains one *mixolide* and half a molecule of Et_2O. The O-atom of the Et_2O molecule is situated on a special position in the crystal lattice. The triolide molecules are arranged around a screw axis and form channels through the crystal, which accommodate the solvent. These channels allow for fast diffusion of the solvent molecules out off the crystal: the crystals are unstable outside a solvent-saturated atmosphere. Crystals damaged by loss of solvent can be restored by short washing with mother liquor. This means that the triolide lattice has more or less survived the loss of solvent molecules, and that the diffusion of these molecules is reversible – reminiscent of the behavior of zeolites.

The structure solution obtained by direct methods revealed the position of all non-H-atoms of the major component, the monoethyl triolide **1**, and the included Et_2O molecule. During the refinement of the structure, no additional Et group could be detected, and there appeared only one rest-electron-density peak near one of the two Me groups in the difference *Fourier* map. The terminal C-atom of the Et group has a rather large temperature factor/degree of disorder. The minor components, the triolides **2** and **3** with two and three Et groups, respectively, do not seem to have a large influence on the structure. The included solvent molecules were highly disordered so that only one of the possible positions is shown in *Fig. 10*. The host molecules inside the channels are not held in their position by H-bonding, a situation in which statistical disorder is a common phenomenon. The channel housing of the solvent molecules must be chiral – only (*R,R,R*)-triolides form it! – and, therefore, enantiomeric molecules might be selectively included.

As described in *Sect. 2.7*, we also prepared a *mixolide* from *Biopol* (81% 3-HB/19% 3-HV) and 3-HV (**13**; total content of 3-HV units 66.7%) to give a mixture containing **A**

(2%), **1** (20%), **2** (46%), and **3** (32%). Again, crystals could be prepared (from Et_2O solution) which were suitable for an X-ray analysis. The structure could be refined to an *R* factor of 0.083 (see *Table 3* and *Fig. 11*). The space group is the same ($C222_1$) as for the *mixolide* with smaller fraction of Et groups. Also, the arrangement of the molecules within the lattice is almost identical, with one Me group being replaced – statistically speaking – by an Et group. This additional Et group points into the channel region which is occupied by solvent molecules, and, consequently, there are less Et_2O molecules present per triolide (1:4) than in the other structure (1:2).

3.5. *Crystallization and X-Ray Crystal-Structure Analysis of a Na^+ Complex of the 3-HV Triolide* **3**. As already mentioned above, we have so far not obtained crystals of the

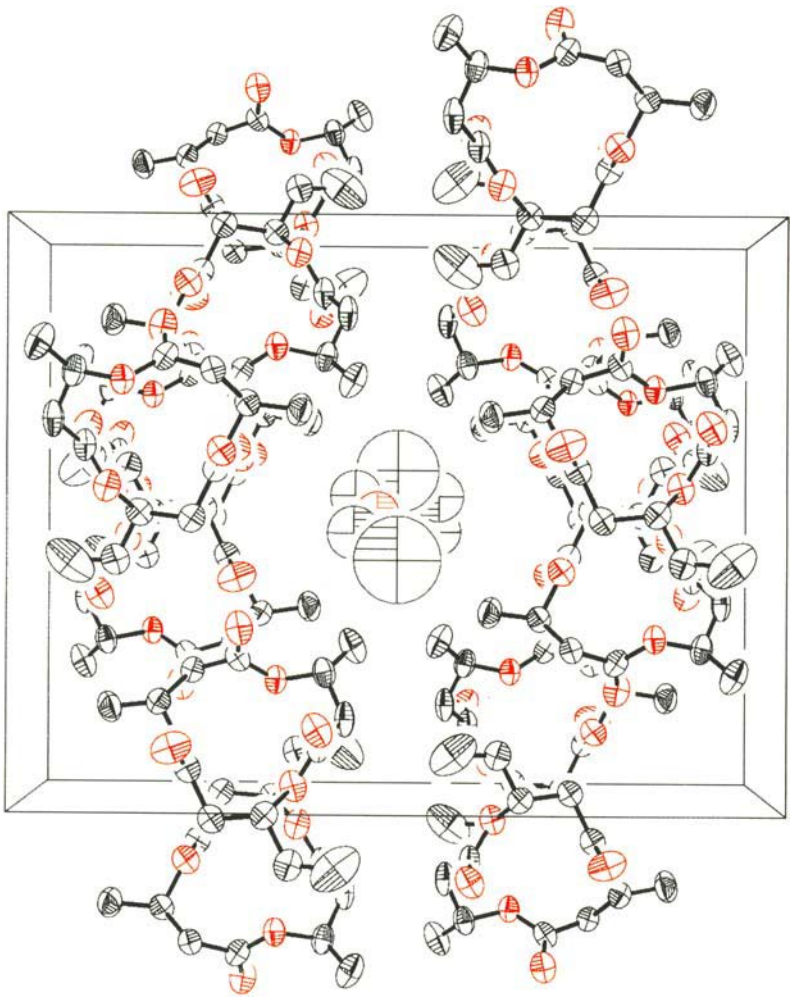

Fig. 10. *Packing plot of the* mixolide *27% 3-HV crystal structure, containing 0.5 equiv. of Et_2O.* Projection down the *c*-axis. O-Atoms are indicated in red, C-atoms in black. Vibrational ellipsoides for the non-H-atoms are drawn for clarity only at the 25% probability level. Rest-electron-density peaks have been omitted for the same reason.

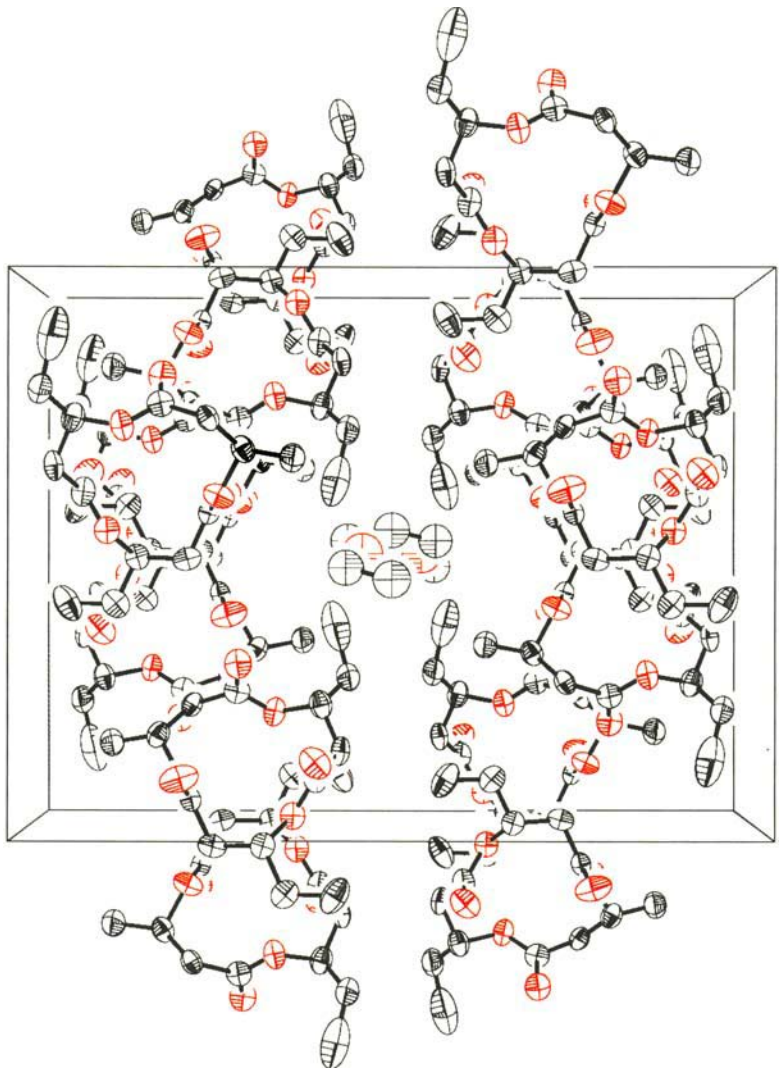

Fig. 11. *Packing plot of the* mixolide *67% 3-HV crystal structure, containing 0.25 equiv. of* Et_2O. Projection down the *c*-axis. O-Atoms are indicated in red, C-atoms in black. Vibrational ellipsoides for the non-H-atoms are drawn at the 25% probability level for clarity. Rest-electron-density peaks have been omitted for the same reason. The Et_2O molecules appear to have smaller vibrational ellipsoides, because the position is only semi-occupied.

triethyl triolide **3** suitable for X-ray analysis. Most remarkably, 'impure' samples containing mixtures of Me- and Et-substituted triolides gave crystals of sufficient quality (see *Figs. 10* and *11*). We have gathered structural information about the elusive triolide **3** in another indirect way: a complex of **3** with NaSCN crystallized from MeCN in a moisture-saturated atmosphere as (**3** · NaSCN · $2H_2O$ · 0.5 MeCN), the crystal structure of which could be determined ($R = 0.055$; see *Tables 3* and *6*, and *Figs. 12* and *13*). This

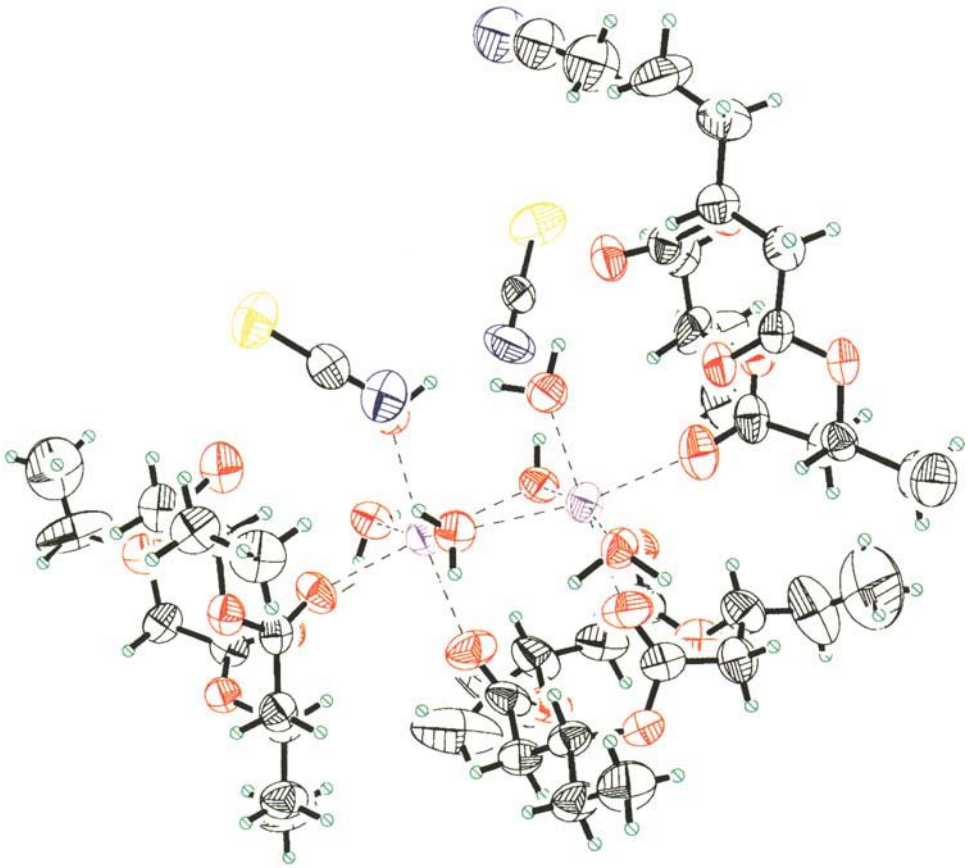

Fig. 12. *ORTEP Representation of the crystal structure of the Na complex* ($C_{15}H_{24}O_6 \cdot NaSCN \cdot 2H_2O \cdot 0.5\ MeCN$). Na^+ Ions are indicated in purple, S-atoms in yellow, O-atoms in red, N-atoms in blue, C-atoms in black, H-atoms in green. Vibrational ellipsoides for the non-H-atoms are drawn at the 50% probability level. The Na^+ ions are shown with their saturated coordination sphere.

structure is interesting in its own right, because it enables a comparison with analogous complexes of the trimethyl-substituted triolide **A** with the thiocyanides of Na^+, K^+, and Ba^{2+} [8] [25]. Furthermore, *c*-P(3-HB), a complex of which with Ca polyphosphate can be extracted from the cell membranes of genetically transformable *E. coli*, may contain a few percent 3-HV [10]; thus, any type of structural information about the interaction of such 3-HV units with cations might be of biochemical relevance.

The asymmetric unit of the Na^+ complex of **3** contains two triolide **3**, two NaSCN, four H_2O, and one MeCN moieties (*Fig. 12*). As can be seen from *Fig. 12*, both Na^+ cations are hexacoordinated; they are bridged by two H_2O molecules and by one triolide **3**. The octahedral coordination spheres are completed by two more H_2O molecules which are bridging the symmetry-equivalent Na^+ ions. This bridging leads to a one-dimensional polymeric structure (*Fig. 13, a*). These immobilized H_2O molecules cause an unfavorable entropy term [30] which must be compensated by the enthalpy of the Na-O coordination

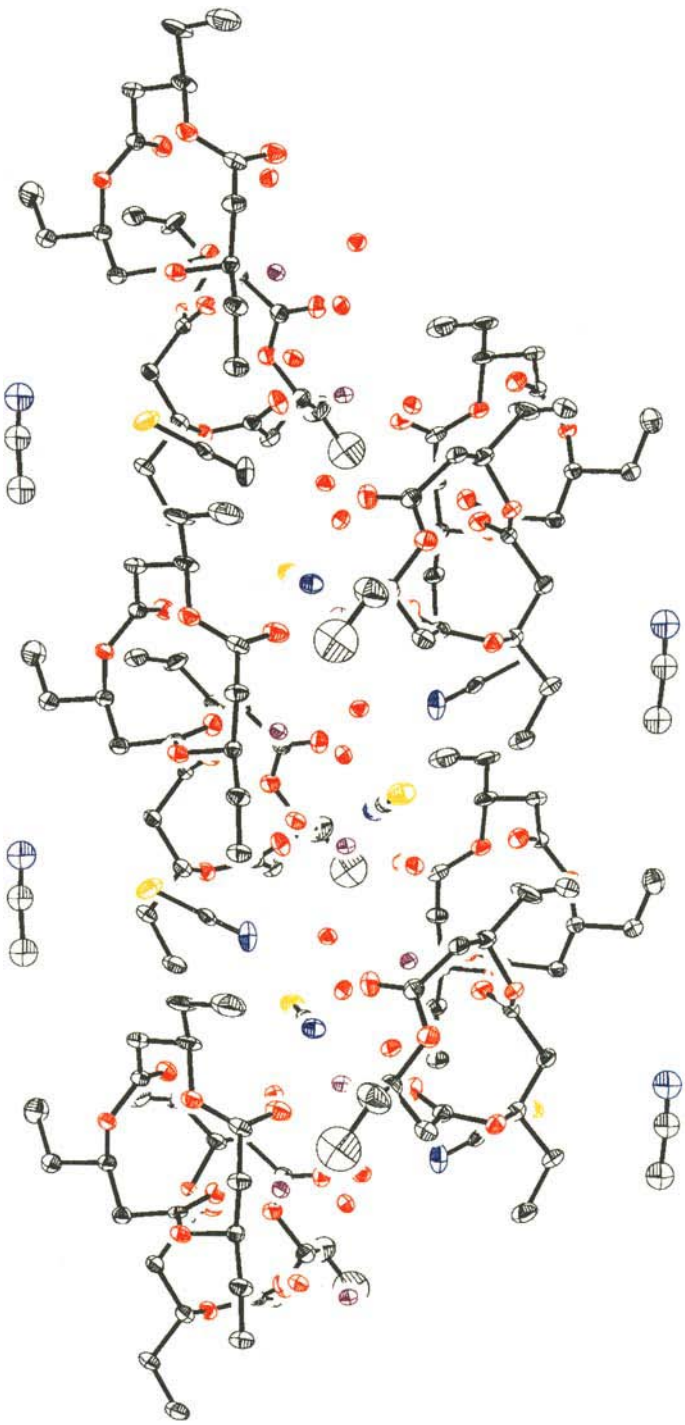

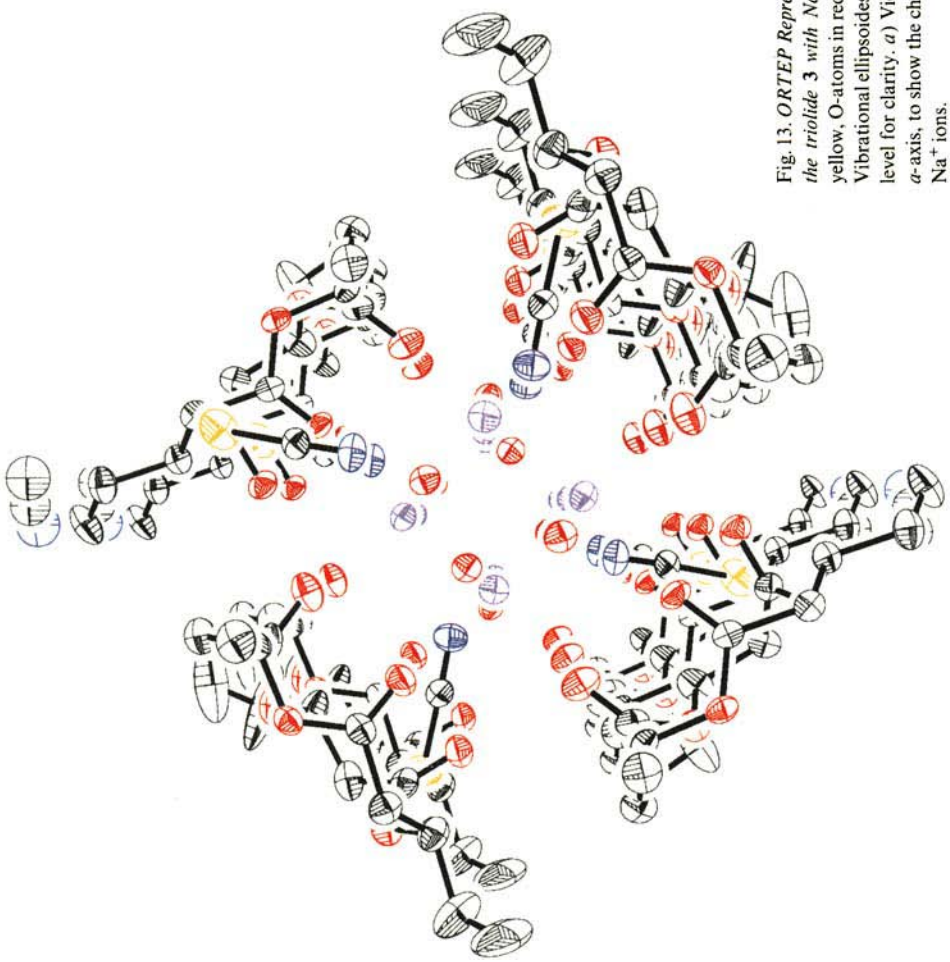

Fig. 13. *ORTEP Representation of the polymeric structure in the Na complex of the triolide* **3** *with NaSCN.* Na^+ Ions are indicated in purple, S-atoms in yellow, O-atoms in red, N-atoms in blue, C-atoms in black, H-atoms in green. Vibrational ellipsoides for the non-H-atoms are drawn at the 25% probability level for clarity. *a*) View perpendicular to the *a*-axis. *b*) Projection along the *a*-axis, to show the channel formed by the triolides **3** around the coordinated Na^+ ions.

Table 6. *Geometries of Complexation of the Na^+ Ions and of Water H-Atoms with the Triolide* **3** *C=O Groups.* The angles α and β are defined as indicated in the accompanying presentation. The Na^+ ions are not located in the C=O plane but above it. The projection of the metall ion onto the C=O plane generates a C=O–M angle β averaging to 169.5° which is significantly larger than in the Na complex of the 3-HB/triolide **A** (155°) [25]. It is remarkable that in the case of the 3-HV complex the Na^+ cation is not situated over the triolide molecule **3** but outside the ring. The variance of the Na···O=C distances (2.344 Å < s < 2.366 Å) is rather small and the same is true for the β angle.

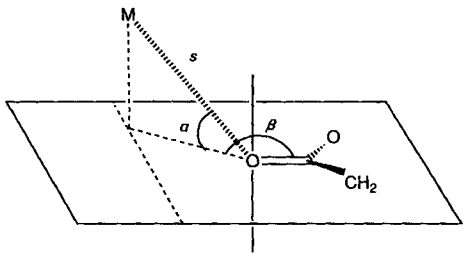

	s [Å]	α [°]	β [°]
Na(1)–O(121)	2.36	15.3	173.1
Na(1)–O(211)	2.36	23.0	171.8
Na(2)–O(131)	2.36	22.0	173.6
Na(2)–O(231)	2.34	10.0	159.6
H(2Ob)–O(111)	1.96	38.7	162.1
H(3Oa)–O(221)	2.05	41.0	176.3

and of the H-bonds. The counterions SCN^- are separated from Na^+ by H_2O molecules (solvent-separated ion pairs). Only two of the three carbonyl O-atoms of each triolide **3** are coordinated to Na^+ in such a way that pairs of Na^+ ions are connected *via* a triolide **3**; the third carbonyl O-atom forms a H-bond with a bridging H_2O molecule. The MeCN molecules are neither coordinated to Na^+, nor do they form H-bonds (clathrate-type inclusion). Despite this, MeCN has a well defined position in the crystal lattice and causes no disorder (see *Fig. 13, a*).

The two crystallographically independent triolide molecules **3** in the NaSCN complex have exactly the same backbone, including the carbonyl groups, but differ in the position of one Et group. Furthermore, the conformation of **3** as present in this structure is very similar to that found in 3-HB-triolide-**A** salt complexes [8] [25][8]). In contrast, the type of complexation between the Na^+ ions and the triolide molecules **A** in the 3-HB-triolide **A** NaSCN complex (4**A**·3NaSCN) [8] [25] and in the new complex (2 **3**·2 NaSCN·4 H_2O·MeCN) differs remarkably: there is no ester-crown, no chelated eight-membered ring, and no double coordination of two Na^+ ions to the same carbonyl O-atom in the complex of **3**. Consequently, the average position of the Na^+ ions with respect to the carbonyl plane is different (*Table 6*)[9]). This difference between the two complexes is probably due to the presence of H_2O molecules which serve as ligands on Na^+ in the complex of **3**. The need for inclusion of H_2O, in turn, might be due to the fact that the more bulky Et-substituted triolide molecules **3** can not move close enough together in order to fill the Na^+-ion coordination sphere properly. The position, with respect to the carbonyl plane, of the H-atoms of those H_2O molecules forming a H-bond to one of the triolide carbonyl O-atoms is similar to that of the Na^+ ions (*Table 6*). The

[8]) *Cf.* the superposition in Fig. 5, a–d in [8].

[9]) *Cf.* the data in *Table 6* with those of the Table in [8].

type of H-bonding between H_2O molecules and ester groups observed here is reminiscent of the situation in peptides [31].

Another interesting feature of the NaSCN complex of triolide **3** is the position of the SCN^- anions. Their N-atoms are surrounded by three H-atoms, with the H_2O molecules forming either bridges to the carbonyl O-atoms (N···H–O–H···O=C) or to another anion (N···H–O–H···N); in addition, all the O-atoms are coordinated to Na^+ ions.

As can be seen from the projection along the *a*-axis shown in *Fig. 13, b*, the crystal structure of the NaSCN complex of **3** contains a kind of channel formed by triolide molecules **3**. The inner surface of this channel is covered by carbonyl O-atoms and thiocyanate N-atoms, and the channel is filled with H_2O molecules and Na^+ ions. The outer surface of the channel is non-polar. Thus, this structure, like those of the previously described complexes [8] [25], may be considered as a model for the proposed [1] [5] [7] cellular ion channel formed from *c*-P(3-HB) and $Ca \cdot PP_i$. A conceptually new aspect, hitherto not discussed in connection with ion-channel formation involving 3-HB oligomers, is the presence of H_2O molecules as 'cement' holding the components together. Inclusion of H_2O in such a channel structure will increase the number of donor ligands available for complexation of cations – so far only the counter ions and the carbonyl O-atoms were assumed to be present [5] [7]. Thus, missing O donor atoms for providing eight ligands to each Ca^{2+} in the recently proposed channel structure for *c*-P(3-HB)·PP_i·0.5 Ca^{2+} [7] could be provided by H_2O molecules, rather than by energetically unfavorable distortions of the P(3-HB) backbone.

We thank the *Stiftung Stipendienfonds*, Germany, for scholarships granted to *T.H.* and *F.N.M.K.*, and also *B. Brandenberger, M. Sperl* (NMR service), and Dr. *W. Amrein, R. Häfliger, O. Greter* (MS service) for the measurement of the spectra. We gratefully acknowledge generous supply of P(3-HB) and *Biopol* from *Zeneca Bio Products*, a company of the *ICI* group, Billingham, England [4].

Experimental Part

1. *General.* All solvents were either *puriss p.A.* quality or distilled over appropriate drying agents. THF was freshly distilled from sodium-benzophenone. NaSCN was from *Fluka AG* and was of *purum* quality. TLC: *Merck-TLC-F_{254}* pre-coated glass plates; detection by immersing in an iodine bath (30 g of I_2, 2 g of KI, in 400 ml of EtOH/H_2O 1:1) and warming. Flash chromatography (FC): silica gel *60* (*Merck*) 40–60 μm. Medium-pressure liquid chromatography (MPLC): *Büchi* system *B-680*. High-pressure liquid chromatography (HPLC): Anal. HPLC was performed on a *Kontron* HPLC system (UV detector *Uvikon LCD-75, Programmer 200,* integrator *Shimadzu C-R 1B Chromatopak*) using a *Knauer* column (*LiChrosorb Si 100,* 7 μm). Prep. HPLC: on a *Knauer* HPLC system (pumb *Typ 64, Programmer 50,* UV detector (*variable-wavelength monitor*)) using a *Knauer* column (*LiChrosorb Si 60,* 7 μm). M.p.: *Büchi 510*; not corrected. Specific rotation: *Perkin-Elmer 241* polarimeter. IR: *Perkin-Elmer-297* spectrometer; in KBr or $CHCl_3$ soln. ^1H- and ^{13}C-NMR: *Bruker WH-300* or *Bruker AM-400*. All spectra were recorded using $CDCl_3$ as solvent and TMS as internal standard. Chemical shifts are given in ppm relative to TMS and coupling constants are given in Hz. Quantitative ^{13}C-NMR (100 MHz) of the carbonyl region (169–171 ppm) of oligolide mixtures: inverse-gated experiment, relaxation delay 3 s, acquisition time 3.2 s, pulse angle 45°. MS: liquid-secondary-ionization (LSI-MS): *VG-ZAB2-SEQ* with 3-nitrobenzyl alcohol. Elemental analysis and osmometric molecular-weight determination: Microanalytical Laboratory of the ETH-Zürich.

2. *(R)-3-Hydroxypentanoic Acid* (**13**). A suspension of 100 g (1.11 mol) of *Biopol* (73% (*R*)-3-hydroxybutanoic acid/27% **13**), in 1000 ml of 1,2-dichloroethane was heated at reflux for 1 h. A soln. of 20 ml of conc. H_2SO_4 in 400 ml of abs. MeOH was added, and the mixture was heated at reflux for 3 d. The clear soln. was cooled to r.t., and 200 ml of half-sat. NaCl soln. were added. After 10 min stirring at r.t., the layers were separated and the aq. layer was extracted three times with 400 ml of $CHCl_3$. The combined org. layers were washed with 200-ml portions of sat. $NaHCO_3$ soln., sat. NaCl soln., dried ($MgSO_4$), evaporated, and distilled (85–105°/15 Torr) to give 94–97 g

(77–80%) of a mixture, containing methyl (*R*)-3-hydroxybutanoate (73%) and methyl (*R*)-3-hydroxypentanoate (27%). These were separated by the use of a *Spaltrohrkolonne* (oil bath: 82–95°, flask: 80–90°, mantle: 75–87°, head: 77–88°, reflux ratio: 20:1 to 10:1, pressure: 15 Torr) to yield 64.9–66.9 g (65–67%) of pure methyl (*R*)-3-hydroxybutanoate and 21.6–22.3 g (61–63%) of pure methyl (*R*)-3-hydroxypentanoate.

To a stirred soln. of 22.4 g (0.4 mol) of KOH in 480 ml of H_2O were added 26.4 g (0.2 mol) of methyl (*R*)-3-hydroxypentanoate and stirred for 24 h at r.t. The alkaline soln. was washed three times with 100 ml of Et_2O, acidified with conc. HCl (pH 1), saturated with NaCl, and extracted five times with 500 ml of Et_2O. The combined org. layers were dried ($MgSO_4$), evaporated, and distilled (120–140°/0.1 Torr) to give 21.3–22.1 g (90.1–93.5%) of **13**.

3. Yamaguchi's *Macrolactonization*. To a stirred soln. of 4.73 g (40 mmol) of **13** in 20 ml of THF at 0° under Ar were slowly added 8.38 g (40 mmol) of 2,6-dichlorobenzoyl chloride and 5.0 g (64 mmol) of pyridine. After 30 min, the ice-bath was removed, and the temp. was allowed to rise within 1.5 h to r.t. The suspension was filtered under Ar and the filtrate diluted with 20 ml of toluene. This soln. was added over a period of 8 h (with a motor-driven syringe) under Ar to a vigorously stirred soln. of 10.0 g (82 mmol) of 4-(dimethylamino)pyridine in 600 ml of toluene at r.t. or 600 ml of refluxing benzene and maintained at this temp. for additional 15 h or 60 h. The mixture then was washed with 200-ml portions of 1N HCl, sat. $NaHCO_3$ soln., and sat. NaCl soln., dried ($MgSO_4$), and evaporated. From these crude product mixtures, the quant. ^{13}C-NMR (100 MHz) spectra of the carbonyl region and the LSI-MS were recorded. The crude product was separated by FC or by the use of a *Stufensäule* (*ca.* 350 g of SiO_2, pentane/Et_2O 2:1). Separation of the mixed fractions: **3**/**5**, FC (SiO_2; toluene/Et_2O 3:1); **4**/**6**, either FC (SiO_2; CH_2Cl_2/Et_2O 3:1) or repeated fractional crystallization from hexanes/CH_2Cl_2 10:1; **7**/**8**, either repeated MPLC (SiO_2; CH_2Cl_2/pentane/Et_2O 10:2:1) or HPLC (SiO_2; hexanes/i-PrOH 99.3:0.7); **9**/**10**, **10**/**11**, and **11**/**12**, repeated FC (SiO_2; pentane/Et_2O 1:1).

After 15 h in toluene at r.t.: 3.1–3.2 g (78–80%) of crude product. ^{13}C-NMR (100 MHz, carbonyl region): **3** (170.41, 2%); **4** (170.05, 3%); **5** (169.70, 35%); **6** (169.65, 27%); **7** (169.60, 15%); **8** (169.55, 8%); **9** (169.53, 4%); **10** (169.51, 3%); **11** (169.50, 2%); **12** (169.49, 1%). Separation by FC/HPLC yielded 500 mg (12.5%) of **5**, 520 mg (13%) of **6**, 300 mg (7.5%) of **7**, 160 mg (4%) of **8**, 100 mg (2.5%) of **9**, 90 mg (2.2%) of **10**, 60 mg (1.5%) of **11**, and 40 mg (1%) of **12**.

After 60 h in benzene at reflux: 1.3–1.4 g (33–35%) of crude product. ^{13}C-NMR (100 MHz, carbonyl region): **3** (170.42, 4%); **4** (170.06, 9%); **5** (169.71, 46%); **6** (169.66, 24%); **7** (169.61, 7%); **8** (169.56, 5%); **9** (169.54, 3%); **10** (169.51, 2%). The macrolides were not isolated.

4. *Macrolactonization with DCC*. To a stirred soln. of 9.45 g (80 mmol) of **13** in 700 ml of CCl_4 at 0° was rapidly added a (to 0° pre-cooled) soln. of 18.16 g (88 mmol) of DCC and 1.19 g (8 mmol) of 4-pyrrolidinopyridine in 100 ml of CCl_4. After 24 h, the suspension was filtered and the filtrate washed with 250-ml portions of sat. $NaHCO_3$ soln. and sat. NaCl soln., dried ($MgSO_4$), and evaporated: 7.1–7.2 g (89–90%) of a colorless oil. From this crude product mixture, the quantitative ^{13}C-NMR (100 MHz) spectrum of the carbonyl region and the LSI-MS were recorded. ^{13}C-NMR (100 MHz, carbonyl region): **5** (169.65, 11%); **6** (169.60, 27%); **7** (169.55, 20%); **8** (169.50, 14%); **9** (169.48, 9%); **10** (169.45, 8%); **11** (169.44, 6%); **12** (169.43, 5%). The oligolide mixture was separated analogously to the procedure described in *3* and led to 510 mg (6.4%) of **5**, 1.17 g (16.3%) of **6**, 760 mg (9.5%) of **7**, 540 mg (6.8%) of **8**, 350 mg (4.4%) of **9**, 200 mg (2.5%) of **10**, 150 mg (1.9%) of **11**, and 120 mg (1.5%) of **12**.

All other reactions shown in *Table 1* were carried out in the same manner considering the variation of temp., concentration, catalyst, and activating reagent. The macrolides from these runs were not isolated.

5. *Acid-Catalyzed Macrolactonization*. A soln. of 11.80 g (0.1 mol) of **13** and 9.51 g (50 mmol) of $TsOH \cdot H_2O$ in 1200 ml of benzene or 1200 ml of toluene/1,2-dichloroethane 4:1 was heated and stirred at reflux for 6 h. Then, H_2O was removed azeotropically with a *Dean-Stark* trap for additional 42 h. The clear brown soln. was cooled to r.t., washed with 250-ml portions of half-sat. Na_2CO_3 soln. and sat. NaCl soln., dried ($MgSO_4$), and evaporated. Of this oligolide mixture, the quant. ^{13}C-NMR (100 MHz) spectrum of the carbonyl region and the LSI-MS were recorded. The semisolid crude product was distilled (150°/0.05 Torr) and the residue separated by FC in analogy to the procedure described in *3*.

In benzene at reflux: 9.7–9.8 g (97–98%) of crude product. ^{13}C-NMR (100 MHz, carbonyl region): **3** (170.38, 40%); **4** (170.03, 20%); **5** (169.67, 20%); **6** (169.62, 10%); **7** (169.57, 5%); **8** (169.52, 3%); **9** (169.50, 2%). Distillation (150°/0.05 Torr) and recrystallization from pentane yielded 3.28 g (32.8%) of **3**. Separation of the residue by FC led to 1.39 g (13.9%) of **4**, 1.53 g (15.3%) of **5**, and 460 mg (4.6%) of **6**.

In toluene/1,2-dichloroethane 4:1 at reflux: 6.4–6.5 g (64–65%) of crude product. ^{13}C-NMR (100 MHz, carbonyl region): **3** (170.35, 56%); **4** (169.99, 11%); **5** (169.64, 18%); **6** (169.58, 8%); **7** (169.54, 4%); **8** (169.49,

2%); **9** (169.47, 1%). Distillation (150°/0.05 Torr) and recrystallization from pentane yielded 3.60 g (36.0%) of **3**. In this run, the other oligolides were not isolated.

6. *(4R,8R,12R)-4-Ethyl-8,12-dimethyl-1,5,9-trioxacyclododecane-2,6,10-trione* (**1**) *and (4R,8R,12R)-4,8-Diethyl-12-methyl-1,5,9-trioxacyclododecane-2,6,10-trione* (**2**): *Mixolide* 27% 3-HV was prepared as described in *5* with 36 g (0.4 mol) of *Biopol* (73% 3-HB/27% 3-HV) and 15.5 g (81 mmol) of $TsOH \cdot H_2O$ in 750 ml of toluene/1,2-dichloroethane 4:1 at reflux for 24 h. Bulb-to-bulb distillation of the residue and recrystallization from pentane/Et_2O 1:1 gave 12.0 g (33%) of a mixture **A**/**1**/**2**/**3**. A single crystal was dissolved in $CDCl_3$ and its composition was analyzed by ^{1}H-NMR. It turned out that the crystal contained 0.4 equiv. of Et_2O per triolide which is in good agreement with the X-ray structure analysis.

^{13}C-NMR (100 MHz, carbonyl region): **A** (169.94, 38%); **1** (170.22, 170.11, 169.91, 44%); **2** (170.37, 170.20, 170.08, 16%); **3** (170.35, 2%). *Mixolide* 67% 3-HV was prepared as described above with 7.0 g (0.78 mol) of *Biopol* (73% 3-HB/27% 3-HV), 11.8 g (0.1 mol) of **13**, and 8.0 g (42 mmol) of $TsOH \cdot H_2O$ in 400 ml toluene/1,2-dichloroethane 3:1 to yield 6.1 g (35%) of a mixture **A**/**1**/**2**/**3**. A single crystal was dissolved in $CDCl_3$ and its composition was analyzed by ^{1}H-NMR. It turned out that the crystal contained 0.2 equiv. of Et_2O per triolide which is in good agreement with the X-ray structure analysis. ^{13}C-NMR (100 MHz, carbonyl region): **A** (169.94, 2%); **1** (170.23, 170.12, 169.92, 20%); **2** (170.38, 170.21, 170.08, 46%); **3** (170.35, 32%).

Mixolide 27% 3-HV (1.5 g) containing **A**/**1**/**2**/**3** was separated by repeated FC (*ca.* 200 g of SiO_2; pentane/Et_2O 3:1) to yield 360 mg (7.9%) of **1** and 150 mg (3.1%) of **2**.

7. *Analytical Data of Macrocycles* **1**–**12**. *Compound* **1**. M.p. 57.0–58.0°. $[\alpha]_D = -17.3$ ($c = 0.925$, CH_2Cl_2). IR ($CHCl_3$): 2974*m*, 2881*w*, 1748*vs*, 1383*s*, 1304*s*, 1267*m*, 1178*s*, 1134*m*, 981*m*. ^{1}H-NMR (300 MHz): 5.42–5.22 (*m*, 2 MeC*H*O, EtC*H*O); 2.65–2.39 (*AB* of *ABX*, CH_2); 1.75–1.57 (*m*, CH_3CH_2); 1.32 (*d*, $J = 6.36$, Me); 1.31 (*d*, $J = 6.35$, Me); 0.92 (*t*, $J = 7.46$, CH_3CH_2). ^{13}C-NMR (75 MHz): 170.28; 170.17; 169.98; 73.13; 69.04; 68.90; 42.21; 41.97; 40.08; 27.79; 20.91; 20.60; 9.39. EI-MS: 272.3 (0.1, M^+), 254.3 (0.2, $[M - H_2O]^+$). Anal. calc. for $C_{13}H_{20}O_6$: C 57.34, H 7.40; found: C 57.57, H 7.27.

Compound **2**. M.p. 72.5–73.0°. $[\alpha]_D = -14.0$ ($c = 0.885$, CH_2Cl_2). IR ($CHCl_3$): 2973*m*, 2882*w*, 1746*vs*, 1373*m*, 1301*s*, 1269*s*, 1179*vs*, 1128*m*, 974*m*. ^{1}H-NMR (500 MHz): 5.38–5.21 (*m*, 2 EtC*H*O, MeC*H*O); 2.60–2.43 (*AB* of *ABX*, CH_2); 1.73–1.57 (*m*, 2 CH_3CH_2); 1.31 (*d*, $J = 6.35$, Me); 0.92 (*t*, $J = 7.47$, CH_3CH_2); 0.91 (*t*, $J = 7.47$, CH_3CH_2). ^{13}C-NMR (125 MHz): 170.46; 170.29; 170.16; 73.23; 73.10; 69.11; 42.02; 40.12; 39.81; 27.90; 27.64; 20.78; 9.42; 9.37. EI-MS: 287.2 (1.2, $[M + H]^+$), 268.2 (1.4, $[M - H_2O]^+$). Anal. calc. for $C_{14}H_{22}O_6$: C 58.73, H 7.74; found: C 58.79, H 7.50.

(4R,8R,12R)-4,8,12-Triethyl-1,5,9-trioxacyclododecane-2,6,10-trione (**3**). M.p. 98.5–99.0°. $[\alpha]_D = -19.4$ ($c = 1.03$, $CHCl_3$). IR (KBr): 2967*w*, 2880*w*, 1743*vs*, 1385*m*, 1267*m*, 1179*s*, 1126*m*, 965*m*. ^{1}H-NMR (400 MHz): 5.30–5.23 (*m*, EtC*H*O); $\nu_A = 2.56$, $\nu_B = 2.48$ (*AB* of *ABX*, $J_{AB} = 13.38$, $J_{AX} = 11.40$, $J_{BX} = 2.01$, CH_2); 1.73–1.57 (*m*, CH_3CH_2); 0.92 (*t*, $J = 7.50$, CH_3CH_2). ^{13}C-NMR (100 MHz): 170.43; 73.23; 39.84; 27.75; 9.36. LSI-MS: 301.1 (83, $[M + H]^+$), 201.1 (34, $[M - 100 + H]^+$). Anal. calc. for $C_{15}H_{24}O_6$: C 59.98, H 8.05; found: C 59.75, H 8.29. Mol. weight (osmom.): 314.0.

(4R,8R,12R,16R)-4,8,12,16-Tetraethyl-1,5,9,13-tetraoxacyclohexadecane-2,6,10,14-tetrone (**4**). M.p. 36.0–36.5°. $[\alpha]_D = +34.0$ ($c = 1.04$, $CHCl_3$). IR (KBr): 2971*w*, 2942*w*, 2883*w*, 1739*vs*, 1463*m*, 1396*m*, 1288*m*, 1190*s*, 1122*m*, 973*m*. ^{1}H-NMR (400 MHz): 5.16–5.10 (*m*, EtC*H*O); $\nu_A = 2.58$, $\nu_B = 2.51$ (*AB* of *ABX*, $J_{AB} = 15.92$, $J_{AX} = 2.66$, $J_{BX} = 8.51$, CH_2); 1.74–1.58 (*m*, CH_3CH_2); 0.93 (*t*, $J = 7.49$, CH_3CH_2). ^{13}C-NMR (100 MHz): 170.09; 71.99; 38.73; 26.95; 9.42. LSI-MS: 401.2 (85, $[M + H]^+$), 201.1 (41, $[M - 200 + H]^+$). Anal. calc. for $C_{20}H_{32}O_8$: C 59.98, H 8.05; found: C 59.84, H 8.21. Mol. weight (osmom.): 403.6.

(4R,8R,12R,16R,20R)-4,8,12,16,20-Pentaethyl-1,5,9,13,17-pentaoxacycloicosane-2,6,10,14,18-pentone (**5**). M.p. 110.5–111.0°. $[\alpha]_D = +19.8$ ($c = 1.03$, $CHCl_3$). IR (KBr): 2969*w*, 2938*w*, 2881*w*, 1738*vs*, 1462*m*, 1389*m*, 1297*m*, 1185*s*, 1130*m*, 976*m*. ^{1}H-NMR (400 MHz): 5.21–5.14 (*m*, EtC*H*O); $\nu_A = 2.58$, $\nu_B = 2.51$ (*AB* of *ABX*, $J_{AB} = 15.21$, $J_{AX} = 7.89$, $J_{BX} = 5.42$, CH_2); 1.72–1.58 (*m*, CH_3CH_2); 0.92 (*t*, $J = 7.49$, CH_3CH_2). ^{13}C-NMR (100 MHz): 169.73; 71.99; 38.68; 26.75; 9.33. LSI-MS: 501.1 (18, $[M + H]^+$), 201.1 (18, $[M - 300 + H]^+$). Anal. calc. for $C_{25}H_{40}O_{10}$: C 59.98, H 8.05; found: C 59.92, H 8.35. Mol. weight (osmom.): 522.4.

(4R,8R,12R,16R,20R,24R)-4,8,12,16,20,24-Hexaethyl-1,5,9,13,17,21-hexaoxacyclotetracosane-2,6,10,14,18,22-hexone (**6**). M.p. (two conformers) 97.5–98.5° (needles); 82.5–83.0° (cubes). $[\alpha]_D = +19.6$ ($c = 1.07$, $CHCl_3$). IR (KBr): 2972*w*, 1738*vs*, 1389*m*, 1272*m*, 1191*s*, 1119*m*, 972*m*. ^{1}H-NMR (400 MHz): 5.26–5.19 (*m*, EtC*H*O); $\nu_A = 2.60$, $\nu_B = 2.52$ (*AB* of *ABX*, $J_{AB} = 16.00$, $J_{AX} = 8.95$, $J_{BX} = 4.29$, CH_2); 1.66–1.59 (*m*, CH_3CH_2); 0.91 (*t*, $J = 7.49$, CH_3CH_2). ^{13}C-NMR (100 MHz): 169.65; 71.64; 38.40; 26.76; 9.29. LSI-MS: 601.2 (19, $[M + H]^+$), 201.1 (21, $[M - 400 + H]^+$). Anal. calc. for $C_{30}H_{48}O_{12}$: C 59.98, H 8.05; found: C 60.01, H 7.89. Mol. weight (osmom.): 599.3.

(4R,8R,12R,16R,20R,24R,28R)-4,8,12,16,20,24,28-Heptaethyl-1,5,9,13,17,21,25-heptaoxacyclooctacosane-2,6,10,14,18,22,26-heptone (**7**). M.p. 54.0–54.5°. $[\alpha]_D = +13.2$ ($c = 1.17$, $CHCl_3$). IR ($CHCl_3$): 2974*w*, 2939*w*, 2882*w*, 1743*vs*, 1463*m*, 1387*m*, 1271*m*, 1179*s*, 1119*m*, 970*m*. ^{1}H-NMR (300 MHz): 5.26–5.17 (*m*, EtC*H*O); $\nu_A = 2.59$, $\nu_B = 2.54$ (*AB* of *ABX*, $J_{AB} = 15.64$, $J_{AX} = 8.78$, $J_{BX} = 4.48$, CH_2); 1.68–1.58 (*m*, CH_3CH_2); 0.90 (*t*, $J = 7.53$, CH_3CH_2). ^{13}C-NMR (75 MHz): 169.62; 71.83; 38.55; 26.87; 9.32. LSI-MS: 833.3 (3, $[M + Cs]^+$), 701.4 (4, $[M + H]^+$), 201.1 (20, $[M - 500 + H]^+$). Anal. calc. for $C_{35}H_{56}O_{14}$: C 59.98, H 8.05; found: C 59.70, H 7.89. Mol. weight (osmom.): 716.9.

(4R,8R,12R,16R,20R,24R,28R,32R)-4,8,12,16,20,24,28,32-Octaethyl-1,5,9,13,17,21,25,29-octaoxacyclodotriacontane-2,6,10,14,18,22,26,30-octone (**8**). $[\alpha]_D = +15.3$ ($c = 1.04$, $CHCl_3$). IR ($CHCl_3$): 2973*w*, 2940*w*, 2882*w*, 1741*vs*, 1463*m*, 1388*m*, 1272*m*, 1178*s*, 1121*m*, 971*m*. ^{1}H-NMR (300 MHz): 5.23–5.14 (*m*, EtC*H*O); $\nu_A = 2.59$, $\nu_B = 2.53$ (*AB* of *ABX*, $J_{AB} = 15.72$, $J_{AX} = 7.99$, $J_{BX} = 5.11$, CH_2); 1.68–1.58 (*m*, CH_3CH_2); 0.90 (*t*, $J = 7.51$, CH_3CH_2). ^{13}C-NMR (75 MHz): 169.60; 71.87; 38.55; 26.83; 9.32. LSI-MS: 823.5 (4, $[M + Na]^+$), 801.5 (31, $[M + H]^+$), 201.2 (27, $[M - 600 + H]^+$). Anal. calc. for $C_{40}H_{64}O_{16}$: C 59.98, H 8.05; found: C 59.87, H 8.34. Mol. weight (osmom.): 681.5.

(4R,8R,12R,16R,20R,24R,28R,32R,36R)-4,8,12,16,20,24,28,32,36-Nonaethyl-1,5,9,13,17,21,25,29,33-nonaoxacyclohexatriacontane-2,6,10,14,18,22,26,30,34-nonaone (**9**). $[\alpha]_D = +14.5$ ($c = 1.10$, $CHCl_3$). IR ($CHCl_3$): 2974*w*, 2941*w*, 2882*w*, 1742*vs*, 1464*m*, 1387*m*, 1271*m*, 1179*s*, 1121*m*, 971*m*. ^{1}H-NMR (300 MHz): 5.22–5.14 (*m*, EtC*H*O); $\nu_A = 2.58$, $\nu_B = 2.53$ (*AB* of *ABX*, $J_{AB} = 15.70$, $J_{AX} = 7.84$, $J_{BX} = 5.22$, CH_2); 1.69–1.59 (*m*, CH_3CH_2); 0.90 (*t*, $J = 7.52$, CH_3CH_2). ^{13}C-NMR (75 MHz): 169.56; 71.87; 38.57; 26.81; 9.32. LSI-MS: 901.4 (13, $[M + H]^+$), 301.1 (12, $[M - 600 + H]^+$), 201.1 (28, $[M - 700 + H]^+$). Anal. calc. for $C_{45}H_{72}O_{18}$: C 59.98, H 8.05; found: C 60.02, H 8.00. Mol. weight (osmom.): 1062.1.

(4R,8R,12R,16R,20R,24R,28R,32R,36R,40R)-4,8,12,16,20,24,28,32,36,40-Decaethyl-1,5,9,13,17,21,25,29,33,37-decaoxacyclotetracontane-2,6,10,14,18,22,26,30,34,38-decaone (**10**). $[\alpha]_D = +13.9$ ($c = 1.02$, $CHCl_3$). IR ($CHCl_3$): 2972*w*, 2941*w*, 2882*w*, 1740*vs*, 1463*m*, 1386*m*, 1272*m*, 1179*s*, 1121*m*, 971*m*. ^{1}H-NMR (300 MHz): 5.22–5.13 (*m*, EtC*H*O); $\nu_A = 2.58$, $\nu_B = 2.53$ (*AB* of *ABX*, $J_{AB} = 15.49$, $J_{AX} = 8.01$, $J_{BX} = 5.02$, CH_2); 1.69–1.59 (*m*, CH_3CH_2); 0.90 (*t*, $J = 7.52$, CH_3CH_2). ^{13}C-NMR (75 MHz): 169.56; 71.90; 38.59; 26.81; 9.32. LSI-MS: 1001.4 (3, $[M + H]^+$), 301.1 (8, $[M - 700 + H]^+$), 201.1 (21, $[M - 800 + H]^+$). Anal. calc. for $C_{50}H_{80}O_{20}$: C 59.98, H 8.05; found: C 60.04, H 8.27. Mol. weight (osmom.): 959.8.

(4R,8R,12R,16R,20R,24R,28R,32R,36R,40R,44R)-4,8,12,16,20,24,28,32,36,40,44-Undecaethyl-1,5,9,13,17,21,25,29,33,37,41-undecaoxacyclotetratetracontane-2,6,10,14,18,22,26,30,34,38,42-undecaone (**11**). $[\alpha]_D = +13.8$ ($c = 0.88$, $CHCl_3$). IR ($CHCl_3$): 2974*w*, 2939*w*, 2881*w*, 1740*vs*, 1463*m*, 1387*m*, 1272*m*, 1179*s*, 1123*m*, 972*m*. ^{1}H-NMR (300 MHz): 5.21–5.13 (*m*, EtC*H*O); $\nu_A = 2.58$, $\nu_B = 2.53$ (*AB* of *ABX*, $J_{AB} = 15.52$, $J_{AX} = 7.87$, $J_{BX} = 5.15$, CH_2); 1.69–1.59 (*m*, CH_3CH_2); 0.90 (*t*, $J = 7.52$, CH_3CH_2). ^{13}C-NMR (75 MHz): 169.53; 71.90; 38.59; 26.80; 9.32. LSI-MS: 1101.4 (4, $[M + H]^+$), 301.1 (10, $[M - 800 + H]^+$), 201.1 (23, $[M - 900 + H]^+$). Anal. calc. for $C_{55}H_{88}O_{22}$: C 59.98, H 8.05; found: C 60.10, H 8.14. Mol. weight (osmom.): 1018.9.

(4R,8R,12R,16R,20R,24R,28R,32R,36R,40R,44R,48R)-4,8,12,16,20,24,28,32,36,40,44,48-Dodecaethyl-1,5,9,13,17,21,25,29,33,37,41,45-dodecaoxacyclooctatetracontane-2,6,10,14,18,22,26,30,34,38,42,46-dodecaone (**12**). $[\alpha]_D = +13.2$ ($c = 1.05$, $CHCl_3$). IR ($CHCl_3$): 2974*w*, 2939*w*, 2882*w*, 1739*vs*, 1463*m*, 1386*m*, 1269*m*, 1179*s*, 1121*m*, 972*m*. ^{1}H-NMR (400 MHz): 5.20–5.13 (*m*, EtC*H*O); $\nu_A = 2.57$, $\nu_B = 2.53$ (*AB* of *ABX*, $J_{AB} = 15.56$, $J_{AX} = 7.70$, $J_{BX} = 5.29$, CH_2); 1.69–1.59 (*m*, CH_3CH_2); 0.90 (*t*, $J = 7.49$, CH_3CH_2). ^{13}C-NMR (100 MHz): 169.53; 71.87; 38.58; 26.77; 9.34. LSI-MS: 1201.4 (2, $[M + H]^+$), 301.1 (10, $[M - 900 + H]^+$), 201.1 (24, $[M - 1000 + H]^+$). Anal. calc. for $C_{60}H_{96}O_{24}$: C 59.98, H 8.05; found: C 60.16, H 8.30. Mol. weight (osmom.): 1526.1.

8. *Bis[(4R,8R,12R)-4,8,12-triethyl-1,5,9-trioxacyclododecane-2,6,10-trione] Bis(sodium thiocyanate) Tetrahydrate Monoacetonitrile Solvate.* A soln. of 300 mg (1 mmol) of **3** and 160 mg (2 mmol) of NaSCN in 1.5 ml of MeCN was heated to reflux for 15 min. The pale yellow clear soln. was allowed to cool to r.t. within 2 h. Isothermic evaporation under a moisture-saturated atmosphere led to slowly growing crystals. These were washed with pentane at −100° to give nearly colorless crystals which decompose within a few minutes at r.t. outside a solvent-saturated atmosphere. They can be stored for several days at −20° with some MeCN. M.p. 59.0–64.5° (dec.). IR (KBr): 3700–3100*m*, 2970*w*, 2933*w*, 2050*vs*, 1740*vs*, 1463w, 1384*m*, 1296*m*, 1270*m*, 1182*s*, 1128*m*, 964*m*.

9. *Crystal-Structure Analysis.* The crystallographic data of the six structures are summarized in *Table 3*. All structures were solved by direct methods using the SHELXS-86 [32] program and refined by full-matrix least-squares analysis with SHELX-76 [33] and SHELX-93 [34].

Tetrolide **4**: $C_{20}H_{32}O_8$. The determination of the cell parameters and the collection of the reflection intensities were performed on an *Enraf-Nonius CAD4* four-circle diffractometer (graphit monochromatized MoK_α radiation,

$\lambda = 0.7107$ Å) at 233 K. C- and O-atoms were refined anisotropically. The H-atoms were added to this structure model with constant isotropic temp. factors on calculated positions and refined using the riding model. The crystal was of poor quality, which explains the rather high *R* factor.

Pentolide **5**: $C_{25}H_{40}O_{10}$. The determination of the cell parameters and the collection of the reflection intensities were performed on an *Picker-Stoe* four-circle diffractometer (graphit monochromatized MoK_α radiation, $\lambda = 0.7107$ Å) at 298 K. C- and O-atoms were refined anisotropically. The H-atoms were added to this structure model with constant isotropic temp. factors on calculated positions and refined using the riding model. Two rest-electron-density peaks near the Me groups of two alkyl substituents were included and refined isotropically.

Hexolide **6**: $C_{30}H_{48}O_{12}$. The determination of the cell parameters and the collection of the reflection intensities were performed on an *Enraf-Nonius CAD4* four-circle diffractometer (graphit monochromatized MoK_α radiation, $\lambda = 0.7107$ Å) at 233 K. C- and O-atoms were refined anisotropically. The H-atoms were added to this structure model with constant isotropic temp. factors on calculated positions and refined using the riding model.

Heptolide **7**: $C_{35}H_{56}O_{14}$. The determination of the cell parameters and the collection of the reflection intensities were performed on an *Enraf-Nonius CAD4* four-circle diffractometer (graphit monochromatized MoK_α radiation, $\lambda = 0.7107$ Å) at 233 K. C- and O-atoms were refined anisotropically. The H-atoms were added to this structure model with constant isotropic temp. factors on calculated positions and refined using the riding model. One of the Et groups showed disorder, and both positions were refined isotropically asuming equal occupation.

Mixolide 27% 3-HV: The determination of the cell parameters and the collection of the reflection intensities were performed on an *Enraf-Nonius CAD4* four-circle diffractometer (graphit monochromatized MoK_α radiation, $\lambda = 0.7107$ Å) at 233 K. C- and O-atoms were refined anisotropically. The H-atoms were added to this structure model with constant isotropic temp. factors on calculated positions and refined using the riding model. The included Et_2O molecules were disordered. The two positions of the O-atoms and for the Me C-atom were constrained to occupy special positions. A rest-electron-density peak was found near C(34) and could be refined isotropically, which means that a small amount of the molecules occupies this position.

Mixolide 67% 3-HV: The determination of the cell parameters and the collection of the reflection intensities were performed on an *Enraf-Nonius CAD4* four-circle diffractometer (graphit monochromatized CuK_α radiation, $\lambda = 1.5418$ Å) at 223 K. C- and O-atoms were refined anisotropically. The H-atoms were added to this structure model with constant isotropic temp. factors on calculated positions and refined using the riding model. The included Et_2O molecules were disordered. The two positions of the O-atoms and for the Me C-atom were constrained to occupy special positions. Two rest-electron-density peaks were found near C(34) and could be refined isotropically. The increased amount of 3-HV units is responsible for the disordered occupation of these positions.

NaSCN-Triolide **3** *Complex:* $C_{15}H_{24}O_6 \cdot NaSCN \cdot 2\,H_2O \cdot 0.5$ MeCN. The determination of the cell parameters and the collection of the reflection intensities were performed on an *Enraf-Nonius CAD4* four-circle diffractometer (graphit monochromatized MoK_α radiation, $\lambda = 0.7107$ Å) at 233 K. Na-, S-, C-, and O-atoms were refined anisotropically, only the C- and N-atoms of the included MeCN were refined isotropically. The H-atoms involved in H-bonding were located from a difference *Fourier* map and refined isotropically. All other H-atoms were added to this structure model with constant isotropic temp. factors on calculated positions and refined using the riding model.

REFERENCES

[1] H.-M. Müller, D. Seebach, *Angew. Chem.* **1993,** *105,* 483; *ibid. Int. Ed.* **1993,** *32,* 477.

[2] *FEMS Microbiol. Rev.* **1992,** 10391.

[3] M. Lemoigne, *Ann. Inst. Pasteur (Paris)* **1925,** *39,* 144; *ibid.* **1927,** *41,* 148; *Bull. Soc. Chim. Biol.* **1926,** *8,* 770.

[4] 'MBL Biopol Natural Thermoplastics. A Guide for Processors', ICI Biological Products, P.O. Box 1, Billingham, Cleveland TS23 1LB, England.

[5] a) R.N. Reusch, T. Hiske, H. Sadoff, *J. Bacteriol.* **1986,** *168,* 553; R. Reusch, T. Hiske, H. Sadoff, T. Harris, T. Beveridge, *Can. J. Microbiol.* **1987,** *33,* 435; b) R.N. Reusch, *FEMS Microbiol. Rev.* **1992,** *103,* 119.

[6] D.A. Plattner, A. Brunner, M. Dobler, H.-M. Müller, W. Petter, P. Zbinden, D. Seebach, *Helv. Chim. Acta* **1993,** *76,* 2004.

[7] D. Seebach, H.M. Bürger, H.-M. Müller, U.D. Lengweiler, A.K. Beck, K.E. Sykes, P.A. Barker, P.J. Barham, *Helv. Chim. Acta* **1994,** *77,* 1099.

[8] D. Seebach, H.M. Bürger, D.A. Plattner, R. Nesper, T. Fässler, *Helv. Chim. Acta* **1993,** *76,* 2581.

[9] H.M. Bürger, D. Seebach, *Helv. Chim. Acta* **1993,** *76,* 2570.

[10] D. Seebach, A. Brunner, H. M. Bürger, J. Schneider, R. N. Reusch, *Eur. J. Biochem.* **1994,** *224,* 317.
[11] D. Seebach, U. Brändli, P. Schnurrenberger, M. Przybylski, *Helv. Chim. Acta* **1988,** *71,* 155.
[12] S. Masamune, G.S. Bates, J.W. Corcoran, *Angew. Chem.* **1977,** *89,* 602; *ibid. Int. Ed.* **1977,** *16,* 585; G. Lukacs, M. Ohno, 'Recent Progress in the Chemical Synthesis of Antibiotics', Springer-Verlag, Heidelberg, 1990.
[13] D. Seebach, A. K. Beck, R. Breitschuh, K. Job, *Org. Synth.* **1992,** *71,* 39.
[14] J. Inanaga, K. Hirata, H. Saeki, T. Katsuka, M. Yamaguchi, *Bull. Chem. Soc. Jpn.* **1979,** *52,* 1989.
[15] J. M. Brown, C. Christodoulou, C. B. Reese, G. Sindona, *J. Chem. Soc., Perkin Trans. 1* **1984,** 1785; P. Sieber, *Tetrahedron Lett.* **1987,** *28,* 6147.
[16] J. Gilbert, T. Kelly, *J. Org. Chem.* **1988,** *53,* 449.
[17] M. Mikolajczyk, P. Kielbasinski, *Tetrahedron* **1981,** *37,* 233.
[18] F. Amat, R. M. Utrilla, A. Olano, *An. Quim.* **1969,** *65,* 829; *Chem. Abstr.* **1970,** *72,* 54840.
[19] B. Neises, W. Steglich, *Angew. Chem.* **1978,** *90,* 556; *ibid. Int. Ed.* **1978,** *17,* 522.
[20] R. B. Woodword, F. E. Bader, H. Bickel, A. J. Frey, R. W. Kierstead, *Tetrahedron* **1958,** *2,* 1.
[21] A. Hassner, V. Alexanian, *Tetrahedron Lett.* **1978,** 4475; G. Höfle, W. Steglich, H. Vorbrüggen, *Angew. Chem.* **1978,** *90,* 602; *ibid. Int. Ed.* **1978,** *90,* 569.
[22] M. Smith, J. G. Moffatt, H. G. Khorana, *J. Am. Chem. Soc.* **1958,** *80,* 6204.
[23] D. F. Mironova, G. F. Dvorko, T. N. Skuratovskaya, *Ukr. Khim. Zh.* **1969,** *35,* 726.
[24] M. Stoll, A. Rouvé, *Helv. Chim. Acta* **1934,** *17,* 1283.
[25] D. Seebach, H.-M. Müller, H.-M. Bürger, D. A. Plattner, *Angew. Chem.* **1992,** *104,* 443; *ibid. Int. Ed.* **1992,** *31,* 434.
[26] G. A. Fischer, J. J. Kabara, *Anal. Biochem.* **1964,** *9,* 303.
[27] D. Seebach, U. Brändli, H.-M. Müller, M. Dobler, M. Egli, M. Przybylski, K. Schneider, *Helv. Chim. Acta* **1989,** *72,* 1704.
[28] M. Yokouchi, Y. Chatani, H. Tadokoro, K. Teranishi, H. Tani, *Polymer* **1973,** *14,* 267.
[29] M. Yokouchi, Y. Chatani, H. Tadokoro, H. Tani, *Polym. J.* **1974,** *6,* 248.
[30] J. D. Dunitz, *Science* **1994,** *264,* 670.
[31] G. A. Jeffrey, W. Saenger, 'Hydrogen Bonding in Biological Structures', Springer Verlag, Berlin, 1991.
[32] G. M. Sheldrick, 'SHELX-86, Program for the Solution of Crystal Structures', University of Göttingen, 1986.
[33] G. M. Sheldrick, 'SHELX-76, Program for Crystal Structures Determination', University of Cambridge, 1976.
[34] G. M. Sheldrick, 'SHELXL-93', *Current Contents (Physical, Chemical and Earth Sciences)* **1989,** *29,* 14.